Thesis for the degree of Doctor of Philosophy

# Glycolytic oscillations in individual yeast cells

**Anna-Karin Gustavsson**

---

Department of Physics
University of Gothenburg
Gothenburg, Sweden 2014

UNIVERSITY OF GOTHENBURG

*Glycolytic oscillations in individual yeast cells*

Anna-Karin Gustavsson
ISBN 978-91-628-9228-9 (printed)
ISBN 978-91-628-9230-2 (electronic)
http://hdl.handle.net/2077/37367

©Anna-Karin Gustavsson, 2014

Cover: Schematic image showing yeast cells being positioned inside a microfluidic flow chamber using optical tweezers.

Department of Physics
University of Gothenburg
SE-412 96 Gothenburg, Sweden
Phone: +46 (0)31-7860000, Fax: +46 (0)31-7861064
http://www.physics.gu.se

Printed by Ale Tryckteam AB
Gothenburg, Sweden 2014

# Glycolytic oscillations in individual yeast cells

Anna-Karin Gustavsson
Department of Physics
University of Gothenburg

## Abstract

Oscillations in the concentration of yeast glycolytic intermediates have been intensively studied since the 1950s, but these studies have so far been limited to observations of average oscillatory behavior in synchronized cultures. Hence, it has remained unknown whether the onset of oscillations is a collective property of the population which requires a high cell density, or if individual cells can oscillate also in isolation. To determine the mechanisms behind oscillations, cell-cell interactions and synchronization, and to investigate the role of cell-cell heterogeneity, oscillations have to be studied on the single-cell level.

The aims of this project were to determine whether individual cells in isolation can oscillate and if there is large heterogeneity among individual cells, to determine if a fluid flow affects the oscillatory behavior, to identify the precise conditions required for oscillations to emerge in individual cells, to investigate the mechanism behind oscillations, and to elucidate the mechanism behind synchronization, its robustness to cell heterogeneity and its universality with respect to different chemical species.

In this work it was shown that glycolytic oscillations can be induced and studied in individual, isolated yeast cells by combining optical tweezers for cell positioning, microfluidics for environmental control and fluorescence microscopy for detection. My single-cell data revealed large heterogeneity and four categories of cell behavior were identified. It was also verified that the oscillatory behavior was determined by the concentrations of glucose and cyanide in the extracellular environment rather than the flow rates used in the microfluidic flow chamber.

Varying the concentrations of glucose and cyanide, the precise conditions for oscillations to emerge in individual cells were determined and it was shown that individual cells can oscillate also at conditions where no oscillations are detected in populations. This indicates that loss of oscillations in a population can be caused by desynchronization rather than by loss of oscillations in individual cells. Investigation of single-cell responses using a detailed kinetic model showed that the onset of oscillations could be described by allosteric regulation of the enzyme phosphofructokinase by AMP and ATP.

To determine the mechanism behind synchronization and to assess its robustness and universality, entrainment of oscillations in individual yeast cells by periodic external perturbations was investigated. It was found that oscillatory cells synchronize through phase shifts and that the mechanism is insensitive to cell heterogeneity (robustness) and similar for different types of external perturbations (universality).

The results presented in this work have advanced our understanding of the complex set of reactions in energy metabolism and the mechanisms through which cells oscillate, communicate, and synchronize. Pursuing these studies will hopefully not only give further information about glycolysis in yeast, but also about energy metabolism, oscillations, and communication in other biological systems, such as oscillatory insulin secretion from islets of $\beta$-cells.

**Keywords**: Optical manipulation, microfluidics, fluorescence microscopy, single cell analysis, *Saccharomyces cerevisiae*, glycolysis, oscillations, NADH, heterogeneity, synchronization, robustness, universality

# Appended Papers

This thesis is based on the work contained in the following scientific papers.

I **Sustained glycolytic oscillations in individual isolated yeast cells**
**A.-K. Gustavsson**, D. D. van Niekerk, C. B. Adiels, F. B. du Preez, M. Goksör and J. L. Snoep
FEBS Journal, **279**, 2837-2847, (2012).

II **Induction of sustained glycolytic oscillations in single yeast cells using microfluidics and optical tweezers**
**A.-K. Gustavsson**, C. B. Adiels and M. Goksör
Proceedings of SPIE, **8458**, 84580Y, (2012).

III **Allosteric regulation of phosphofructokinase controls the emergence of glycolytic oscillations in isolated yeast cells**
**A.-K. Gustavsson**, D. D. van Niekerk, C. B. Adiels, B. Kooi, M. Goksör and J. L. Snoep
FEBS Journal, **281**, 2784-2793, (2014).

IV **Entrainment of heterogeneous metabolic oscillations in single cells**
**A.-K. Gustavsson**, C. B. Adiels, B. Mehlig and M. Goksör
Submitted.

All publications are reprinted by permission of the copyright holders.

My contributions to the appended papers:

**Paper I**: I planned and performed the experiments, the data analysis and the numerical simulations of the microfluidic flow chamber. I wrote the corresponding sections of the paper.

**Paper II**: I planned and performed the experiments, the data analysis and the numerical simulations of the microfluidic flow chamber. I wrote the paper.

**Paper III**: I planned and performed the experiments, the data analysis and the numerical simulations of the concentration distribution within the microfluidic flow chamber without cells. I wrote the corresponding sections of the paper.

**Paper IV**: I planned and performed the experiments and the data analysis. I wrote the paper together with Prof. Mehlig.

# Contents

# Chapter 1

# Introduction

## 1.1 Energy metabolism in yeast

All living organisms require energy to fuel processes inside the cells to allow the cells to grow, reproduce, and respond to their environment. In cells, the energy-rich molecule adenosine triphosphate (ATP) is used as a direct energy source and the purpose of energy metabolism is to produce ATP through the conversion of an indirect energy source such as a glucose molecule.

The first part of energy metabolism is called glycolysis and in this process glucose molecules are converted into pyruvate through a number of enzymatic reactions (Fig. 1.1(a)). For each glucose molecule converted, two adenosine diphosphate (ADP) molecules are phosphorylated to two ATP molecules and two nicotinamide adenine dinucleotide ($NAD^+$) molecules are reduced to two NADH molecules.

If oxygen is present, pyruvate and NADH molecules can be used in aerobic respiration, which occurs inside the mitochondria (Fig. 1.1(b)). Pyruvate is then converted into acetyl-CoA, which enters the citric acid cycle, also known as the Krebs cycle, the Szent-Györgyi-Krebs cycle or the tricarboxylic acid cycle. Here it is used to produce more ATP and NADH. The NADH molecules produced both during glycolysis and in the citric acid cycle are then used in the electron transport chain, where they are oxidized into $NAD^+$. In the transport chain, electrons are transferred through a series of membrane-bound complexes. In this process, protons are transported through the complexes to the intermembrane space of the mitochondrion, creating an electrochemical proton gradient across the inner membrane. When passing through the last complex, called cytochrome *c* oxidase, the electrons bind to oxygen and protons, forming water. Via a membrane-bound enzyme called ATP synthase, the protons are transported back into the inner space of the mitochondrion, producing even more ATP.

If cyanide is added to a cell, it binds to cytochrome *c* oxidase and prevents it from transporting electrons to the oxygen molecules [1]. This stops the electron transport chain and prevents NADH from becoming oxidized, which in turn stops the citric acid cycle. Cells which are solely dependent on aerobic respiration will then die from anoxia. Yeast cells, on the other hand, can survive also in anaerobic conditions, where they instead ferment pyruvate via acetaldehyde (ACA) into ethanol. In this process NADH is also oxidized to $NAD^+$, ensuring that glycolysis can continue. Some cell types, such as *S. cerevisiae*,

prefer to use fermentation also in aerobic conditions, when high concentration of glucose is available. This is known as the Crabtree effect [2].

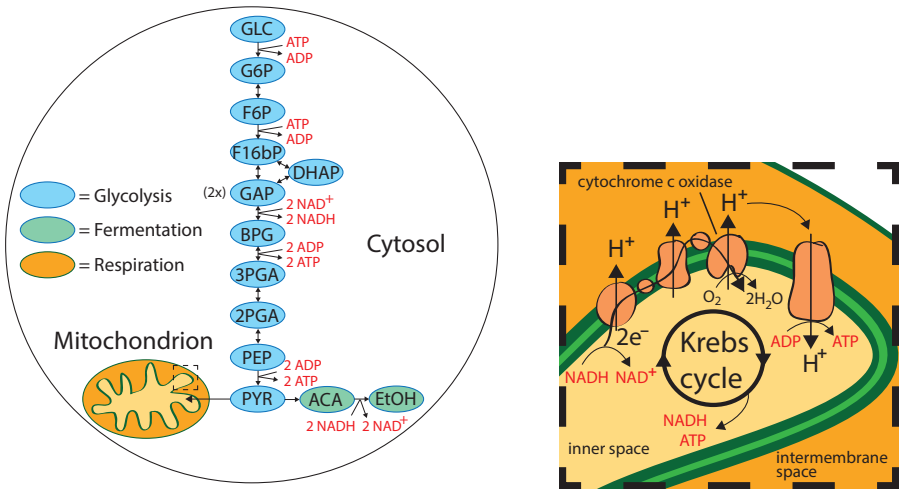


(a) (b)

**Figure 1.1:** (a) Simplified schematic of energy metabolism in yeast. The molecules in blue are involved in glycolysis, while molecules in green are involved in fermentation. If oxygen is present, pyruvate can be converted into acetyl-CoA and used in respiration inside the mitochondrion (yellow). (b) Schematic drawing of respiration within the mitochondrion. acetyl-CoA converted from pyruvate is used in the Krebs cycle, where both NADH and ATP are produced. NADH from glycolysis and from the Krebs cycle is then used to drive the electron transport chain, were even more ATP is produced. If cyanide is added, it binds to a complex in the electron transport chain called cytochrome *c* oxidase and prevents it from transporting electrons to oxygen molecules. This stops the transport chain and since NADH then no longer becomes oxidized into $NAD^+$, the entire respiration stops. Organisms not able to ferment then die from anoxia. GLC, glucose; G6P, glucose 6-phosphate; F6P, fructose 6-phosphate; F16bP, fructose 1,6-bisphosphate; DHAP dihydroxyacetone phosphate; GAP, glyceraldehyde 3-phosphate; BPG, 1,3-bisphosphoglycerate; 3PGA, 3-phosphoglycerate; 2PGA, 2-phosphoglycerate; PEP, phosphoenolpyruvate; PYR, pyruvate; ACA, acetaldehyde; EtOH, ethanol

## 1.2 Glycolytic oscillations in yeast

If yeast cells are exposed to certain concentrations of glucose and cyanide, the concentration of metabolites in glycolysis starts to oscillate. These glycolytic oscillations have been studied since the 1950s, both *in vivo* and *in silico* and both in populations of intact cells and in yeast extracts [3]. In 1957, Duysens and Amesz observed significant fluctuations

in the fluorescence intensity from NADH in suspensions of yeast cells [4]. In later experiments, damped sinusoidal oscillations with 12 full cycles were observed in *Saccharomyces carlsbergensis* [5] and in subsequent studies glycolytic intermediates were also found to be oscillating [6]. It was shown that intact cells in general oscillate with a shorter period time than cell free extracts, with period times of around 30-60 s and several minutes in the two cases respectively [3]. The frequency of the oscillations was shown to depend on both the temperature [5] and on the injection rate of substrates [7–9]. Later it was also shown that the glucose transporter has high control of the frequency in intact cells [10]. This could explain the differences in frequencies found in extracts, where the membrane is ruptured, and in intact cells. It has also been shown that the amplitude of the oscillations depends on temperature [5] and cell density [11] and that the oscillations last longer in high density cell cultures [11–13].

In the 1990s, Richard *et al.* presented a method to induce sustained oscillations in dense populations of intact cells. By harvesting cells at the diauxic shift, where glucose in the medium becomes exhausted, starving the cells for a few hours and subsequently adding glucose and cyanide, sustained macroscopic oscillations could be studied [14, 15]. These oscillations died off first at glucose exhaustion. Cyanide was in these studies added for two reasons; to inhibit respiration and to bind ACA. ACA is an intermediate metabolite which rapidly diffuses across the cell membrane and in dense cell cultures acts as a synchronizing agent for the oscillations [16–20].

In most studies, macroscopic oscillations were detected only for a cyanide concentration range of 2-8 mM [9, 15, 21]. The explanation for using this concentration range was to ensure inhibition of respiration by cyanide binding to cytochrome *c* oxidase [15], and to lower the ACA concentration within a range where the cells are sensitive to ACA secretion from other cells [15–17, 19, 22] by cyanide binding ACA [23]. Even though cyanide might not be present in natural yeast habitats, these conditions resemble those experienced by yeast cells in a dough, where anaerobiosis may occur and ACA is removed by evaporation.

In addition to ACA, other substances have also been shown to cause synchronization of the cell responses, e.g. glucose at concentrations below saturation level [10, 17, 19, 24, 25] and oxygen [26]. Other substances, such as cyanide [17], ethanol [16, 17, 27, 28] and pyruvate [17], were also investigated, but it was found that they give insufficient or no response under the experimental conditions. Even though cyanide perturbations were shown to increase the levels of NADH in the cells, cyanide was discarded as a quencher with the motivation that it has slow reaction with the rest of the system [17].

Although glycolytic oscillations have been intensively studied on the macroscopic level, these studies only revealed information about the population average response. The lack of single-cell studies of this phenomenon has caused many questions to remain unanswered. Limitations of previous macroscopic studies and motivation for using single-cell analysis to solve some of these questions are discussed in Chapter 2.

## 1.3 Glycolytic oscillations in a wider perspective

Glycolytic oscillations have been shown to occur also in other cell types, e.g. muscle extracts [29, 30], heart extracts [31], Ehrlich ascites tumor cells [32] and pancreatic $\beta$-cells [33]. Since glycolytic oscillations also affect the ATP/ADP ratio, they have been proposed

as a key mechanism for pulsatile insulin secretion from $\beta$-cells [34, 35]. One hypothesis is that an increase in the ATP/ADP ratio closes ATP-dependent $K^+$-channels in the plasma membrane of the $\beta$-cells [36]. This leads to membrane depolarization, which in turn opens voltage sensitive $Ca^{2+}$-channels, leading to influx of $Ca^{2+}$ into the cell which triggers exocytosis of insulin. This hypothesis is supported by the fact that changes in ATP/ADP ratio, NADH and oxygen consumption precede the initial rise in $Ca^{2+}$ in glucose-stimulated $\beta$-cells and that no further change can be seen in the metabolic parameters at the rise of $Ca^{2+}$ [37]. Another hypothesis is that the insulin oscillations are caused by $Ca^{2+}$ feedback, where $Ca^{2+}$ activates $K^+$-channels and evokes exocytosis. Recently, these two hypotheses were combined in a "dual oscillator model", including both a slow metabolic component and a fast electrical component, which successfully described much of the data on pulsatile insulin secretion [35].

Understanding the biochemical mechanism of insulin secretion oscillations is very important, since several studies have demonstrated a greater hypoglycemic effect of insulin infused in a pulsatile manner than when infused at a constant rate [38, 39] and that this pulsatility is impaired in humans with type II diabetes [40]. This suggests that type II diabetes may be caused by loss or irregularity of insulin oscillations [41–43]. Studies have also shown that humans with mutations in phosphofructokinase, a glycolytic enzyme known to have large influence on glycolytic oscillations (see Section 4.3), have impaired insulin oscillations [44].

## Chapter 2

# Motivation and Aims

There are several reasons to study glycolytic oscillations in yeast. First, such studies will give detailed information about the complex reaction network in energy metabolism. Since the glycolytic pathway is similar in most organisms, both prokaryotic and eukaryotic, a deeper understanding of the reaction network in yeast will give insight into the function of glycolysis also in other organisms. These studies will also give information about a mechanism of cell-cell communication and synchronization. Cell-cell communication is a prerequisite for organization of communities and, evolutionary, this phenomenon might thus have provided a path from unicellular to multicellular behavior. If the mechanism behind synchronization of glycolytic oscillations is robust with regard to cell heterogeneity and similar for different chemical species, it indicates that the mechanism might be at work also in other cell types, possibly for different metabolic species. Detailed knowledge of glycolytic oscillations in yeast might thus also reveal information about the mechanism behind pulsatile insulin secretion in individual pancreatic $\beta$-cells, how the individual $\beta$-cells communicate and synchronize their secretion in and between islets of Langerhans, and why the pulsatility might become impaired in humans with type II diabetes.

In a population of millions of yeast cells, synchronization is a requirement for studies of oscillations. One question that remained unanswered for a long time is why a population of cells loses its oscillations, as reported for e.g. low glucose concentrations [7, 9] and low cell densities [11–13]. Is it due to the individual cells in the population losing their oscillations or is it due to desynchronization of the oscillations? Another question is whether there is large heterogeneity in the oscillatory behavior on the single-cell level. Several attempts have been made to study oscillations in individual cells, both in a population and in isolation [12, 28, 45, 46]. Early studies indicated heterogeneity in period time on the single cell level and that individual cells continued to oscillate also when the population as a whole did not [12]. However, in more recent studies, individual cells from an oscillating population were investigated without any indications of oscillations [28, 46]. It has been suggested that single cells in isolation might not be able to oscillate and that the onset of oscillations is a collective property and not possible at low cell densities [45].

- The first aim of this work was to answer whether individual cells in isolation can show glycolytic oscillations and to characterize the heterogeneity in response among the individual cells. This was investigated in **Paper I** and is further discussed in Section 4.1.

In the experiments in this work, microfluidics was used to control the extracellular environment [47, 48]. What chemicals the cells were exposed to were controlled by adjustments of the flow rate in the microfluidic flow chamber. Hence, detected cell responses could be caused either by changes in flow rates in the microfluidic chamber or by changes of chemicals in the extracellular milieu. To investigate the mechanism behind the detected cell response, it must be determined whether the responses were due to changes of chemicals or due to changes of flow rates.

- The second aim of this work was to investigate the role of flow rates on the detected cell responses. This study is presented in **Paper II** and discussed in Section 4.2.

Another interesting question to investigate is whether the precise conditions required for oscillations to emerge in individual cells differ from the conditions where synchronized oscillations are detected in populations [9]. Answering this question might further elucidate if the conditions for synchronized oscillations in a population are a subset of the conditions for single cell oscillations and might suggest a new regime of conditions for the study of oscillatory behavior. Investigating the conditions required for oscillations to emerge in individual cells might also give clues to the mechanism responsible for oscillations.

- The third aim of this work was to determine the precise conditions required for oscillations to emerge in individual cells, without any additional requirements of synchronization, and to investigate the mechanism behind oscillations. This is investigated in **Paper III** and discussed in Section 4.3.

The oscillatory behavior detected in a population does not only depend on the oscillatory behavior of the individual cells [49, 50], but also on the cell-cell interactions leading to synchronization. Since observations of macroscopic oscillations do not distinguish between oscillations and synchronization, previous measurements have neither allowed to deduce the microscopic mechanism of synchronization nor how robust this mechanism is to cell heterogeneity [16, 17, 20].

Experimental studies of macroscopic oscillations indicate that phase synchronization may play a role [16]. To quantify the effect, and to unequivocally establish whether synchronization can be achieved by phase changes alone, it is necessary to follow how an individual cell is entrained by a periodic perturbation. To determine whether the frequency and amplitude of the oscillations remain unaffected by the perturbation and how their values before the perturbation affect the propensity of the cell to be entrained when the periodic perturbation is switched on, the frequency and amplitude of the individual cells should be measured both before, during, and after the perturbation. Theoretical models have shown in-phase or out-of-phase synchronization, sensitively depending on model parameters [9]. A very important open question is how the phase of an entrained cell relates to the phase of the perturbation. Do cells typically oscillate in phase with the perturbation or not? Macroscopic experiments do not allow resolving this question, because subpopulations oscillating out-of-phase will only lead to a lowering of the amplitude of the macroscopic signal. To determine the mechanism of synchronization, these experiments must be performed on individual cells.

In a theoretical model for phase synchronization, the efficiency of the mechanism is determined by the heterogeneity of the cells as well as the strength of the entrainment

[51]. This is very important because no two cells are alike, and different cells respond differently to external perturbations. Measuring the macroscopic response it is impossible to distinguish between full and partial synchronization of a population. To determine how robust the synchronization mechanism is with respect to cell heterogeneity, the response of an ensemble of independent individual cells with different properties should be studied.

Entrainment involves the entire glycolytic network, and not just a single reaction or intermediate. The effect might in fact be the result of the combined response to several different chemical species [52]. The kinetics leading to synchronization is thus very complicated, but entrainment appears to occur for a wide range of different conditions and types of perturbations [10, 16–20, 24–26]. Determining the universality of the synchronization mechanism for different chemical species is of great importance for the general understanding of cell-cell communication, and might give clues to how this communication may work in different organisms.

- The fourth aim of this work was to determine the synchronization mechanism, its robustness and its universality. This study is presented in **Paper IV**, and discussed in Section 4.4.

# Chapter 3

# Methodology

## 3.1 Experimental procedures

To induce and study glycolytic oscillations in individual yeast cells, optical tweezers [53–57] were combined with microfluidics [58–61] and fluorescence microscopy. The optical tweezers were used to position yeast cells in arrays with variable cell-cell distance on the bottom of a microfluidic flow chamber. The cell responses were then measured using fluorescence microscopy, while the extracellular environment was controlled and adjusted using the microfluidic flow chamber. This section gives a brief description of the experimental procedures and techniques used, where the focus is on special aspects that must be considered for the experiments in this work. Technical specifications and description of the experimental setup can be found in **Paper I** and detailed information about the specific experimental procedures can be found in **Papers I-IV**.

### 3.1.1 Cell preparation

In my experiments, the budding yeast *S. cerevisiae* (X2180 haploid strain) was used and the cells were prepared as outlined by Richard *et al.* [14, 15]. The cells were grown on a rotary shaker at 30° C and harvested by centrifugation when they reached the diauxic shift, i.e. were the glucose in the medium became exhausted. The glucose concentration was measured using glucose test sticks. Since the lowest levels of glucose the test sticks could measure was 0.1%, the cells were allowed to grow for between 15-30 min after the test sticks showed a negative response to glucose to ensure that glucose was completely depleted. Harvesting cells too early or too late would lead to damped oscillations [14]. The cells were then washed twice in a potassium phosphate buffer and subsequently glucose starved for 3 h at 30° C on a rotary shaker. After starvation, the cells were washed once more in the potassium phosphate buffer and stored on ice or in fridge at 4° C until use. Storing in fridge was to prefer, since less clustering of cells seemed to appear when the cells later were introduced into the microfluidic flow chamber (see Section 3.1.3). To further reduce the amount of clustering, the cells were washed once in room temperature potassium phosphate buffer and vortexed for 15-20 s right before use.

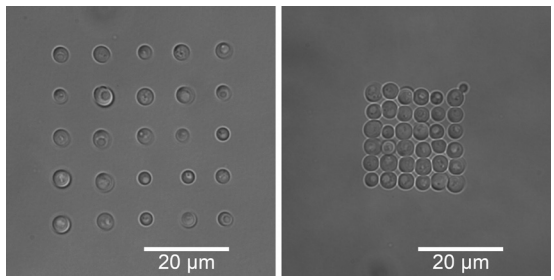


**Figure 3.1:** Brightfield images of yeast cells positioned in sparse (left) and tightly packed (right) arrays using optical tweezers. Since yeast cells can interact it is crucial to control the cell-cell distance during experiments.

### 3.1.2 Optical tweezers for cell positioning

To investigate oscillations from individual cells, the cell responses should be measured during several minutes. In solution, yeast cells will drift due to Brownian motion and due to the fluid flow of the medium. Passive sorting by for instance sedimentation can result in a higher ratio of cells with a specific intrinsic property than what is representative on the population level. Since yeast cells can communicate, it is crucial that the cell-cell distances are well-defined. However, passive sorting will result in arbitrary cell-cell distances. In this work the solution was to use optical tweezers [53–57], where strongly focused laser light was used to directly trap, move and position cells in the measurement region inside a microfluidic flow chamber (Fig. 3.1). The optical tweezers used in this work consisted of a single, stationary trap and was constructed as described by Fällman *et al.* [62]. Optical tweezers can be used to selectively position cells with a desired property for investigation. However, in this work all single cells caught in the trap were used in the experiment, regardless of e.g. cell size or morphology, to ensure that the detected cell responses were representative of the cell population.

The theory used to describe the forces acting on a transparent sphere in an optical trap differs depending on the radius of the sphere, $r$. When $r \ll \lambda$, where $\lambda$ is the wavelength of the laser light in the medium, the forces can be described according to Rayleigh theory [63], and when $r \gg \lambda$, ray optics can be used [64]. It has been shown that when $r \ll \lambda$, the axial trapping efficiency depends on $r^3$ and when $r \gg \lambda$, the axial trapping efficiency is independent of $r$ [65]. In the regime where $r \approx \lambda$, the forces are more difficult to calculate theoretically, but Gouesbet *et al.* have developed a generalized Lorentz-Mie theory which can be used for all sizes and locations of a particle in a Gaussian beam [66]. Even if the theoretical description of optical tweezers varies with particle size, experiments have shown that it is possible to trap particles in the wide size range from 25 nm to 45 $\mu$m [55, 67]. To accurately measure the actual forces on a particle or bead trapped, an experimental force calibration is usually necessary [68].

In experiments with live cells the sensitivity of the cells sets the maximum intensity of the laser light that should be used. Photodamage of cells can be caused directly by heating through absorption or indirectly by generation of free radicals which in turn can cause

harmful chemical reactions. In general, damage by these effects increases and decreases with wavelength respectively, although there can be specific wavelength regions where cells are particularly prone to photochemical damage. To reduce the risk of photodamage near infrared light is usually used instead of visible light [57, 69, 70]. This reduces the risk of photochemical damage, while utilizing a local minimum of the absorption spectrum of water, which is a major heat absorber in cells. In **Papers I-IV** the time the cells were held with the optical tweezers was kept below 5 s to minimize any damaging effects by the laser light. In the setup used in this work, cells were still viable after 10 s of illumination with a 1070 nm laser at an intensity of 240 mW [71].

### 3.1.3 Microfluidics for environmental control

To study how metabolism is affected by changes in the extracellular environment, chemicals in the surroundings need to be controlled and adjusted. Cells usually have high sensitivity to their surroundings and even low concentrations of a substance can cause significant responses [72]. In bulk, it is difficult to reversibly switch between two different media and follow the response from the cells. In this work the solution was to use microfluidics, where fast, reversible changes of the environment can be performed while cell responses are studied under the microscope [58–61]. The microfluidic flow chambers used in **Paper III** and in **Papers I**, **II** and **IV** had three [71] and four inlet channels respectively, and were fabricated as described by Sott *et al.* [61].

In fluid mechanics, the fluid velocity at a given time and position, $\mathbf{u}$, can be calculated from the Navier-Stokes equation, which describes Newton's second law when applied to fluid motion. In this work, all solutions introduced into the microfluidic flow chamber were incompressible and Newtonian, i.e. the densities of the fluids, $\rho$, were independent of the pressure, $p$, and the viscosities of the fluids, $\eta$, were independent of the flow velocity. The Navier-Stokes equation can then be written

$$\rho\left(\frac{\delta\mathbf{u}}{\delta t}+\mathbf{u}\cdot\nabla\mathbf{u}\right)=-\nabla p+\eta\nabla^2\mathbf{u}+\mathbf{f}, \tag{3.1}$$

where $\mathbf{f}$ represents body force densities, such as gravity or centripetal forces [73]. The left-hand side of the equation describes the inertial acceleration, where $\rho\frac{\delta\mathbf{u}}{\delta t}$ and $\rho\mathbf{u}\cdot\nabla\mathbf{u}$ represent temporal and spatial variations of the velocity respectively. The right-hand side of the equation describes the applied force density, where pressure forces are described by $-\nabla p$ and viscous forces are described by $\eta\nabla^2\mathbf{u}$.

An important parameter when working with microfluidic devices is the Reynolds number, which is the ratio between inertial and viscous forces in a flow. The inertial term $\rho\mathbf{u}\cdot\nabla\mathbf{u}$ in Eq. (3.1) is proportional to $\frac{\rho U^2}{L}$, where $U$ and $L$ are the typical velocity and length scales of the chamber. The inertial term $\rho\frac{\delta\mathbf{u}}{\delta t}$ is proportional to $\frac{\rho U}{\tau}$, where $\tau$ is the characteristic time of the variations of the velocity. Setting $\tau$ proportional to $\frac{L}{U}$, the entire inertial acceleration will be proportional to $\frac{\rho U^2}{L}$. The viscous term $\eta\nabla^2\mathbf{u}$ is proportional to $\frac{\eta U}{L^2}$, and taking the ratio between the inertial and the viscous forces, the Reynolds number can be calculated

$$Re = \frac{\mathbf{F}_{inertial}}{\mathbf{F}_{viscous}} = \frac{\left(\frac{\rho U^2}{L}\right)}{\left(\frac{\eta U}{L^2}\right)} = \frac{\rho U L}{\eta}. \tag{3.2}$$

For high Reynolds numbers, inertial forces dominate over viscous forces and the flow becomes turbulent. For lower Reynolds numbers, viscous forces dominate and for Reynolds numbers below 2300, flows are generally considered laminar [74]. In the chambers used, the channels had a rectangular cross section and the typical length scale can then be found from the hydraulic diameter $D_h$

$$L = D_h = \frac{4A}{P}, \tag{3.3}$$

where $A$ is the cross-sectional area and $P$ is the wetted perimeter, i.e. the inner circumference of the channel [75]. Using typical values for the chambers used in this work, with channels that are 100 $\mu$m wide and 27 $\mu$m high and a flow velocity of 2.5 mm/s (a flow rate of approximately 400 nl/min), the Reynolds number is 0.1, when $\rho_{water} \approx 10^3$ kg/m$^3$ and $\eta_{water} \approx 10^{-3}$ Pa·s are used. This value is orders of magnitude below 2300 and the flow in the channels are thus completely laminar.

For low Reynolds numbers, the left-hand side of the Navier-Stokes equation can be neglected. Also body forces are usually negligible compared to the viscous forces and the Navier-Stokes equation can be reduced to Stokes equation

$$\eta \nabla^2 \mathbf{u} = \nabla p. \tag{3.4}$$

It can be seen that Stokes equation is time-independent and laminar flows are thus reversible in time.

To simulate the flows in a microfluidic flow chamber, the Navier-Stokes equation can be combined with the continuity equation [76], here in the form of the equation for mass conservation,

$$\frac{\delta \rho}{\delta t} + \nabla \cdot (\rho \mathbf{u}) = 0. \tag{3.5}$$

Since it is assumed that the fluid is incompressible, the density can be assumed to be constant and the mass conservation equation can be reduced to

$$\nabla \cdot \mathbf{u} = 0. \tag{3.6}$$

The environment within a microfluidic flow chamber is not only determined by the velocity profiles of the flows, but also by the concentration distribution of chemicals. The flux of particles $\mathbf{J}$ from a lower to a higher concentration, $c$, can be described by Fick's law of diffusion [76]

$$\mathbf{J} = -D \nabla c. \tag{3.7}$$

Convection is the particle transport due to fluid flow and the flux of particles due to convection can be expressed $c\mathbf{u}$. Combining the expressions from Fick's law of diffusion and the expression for convection with the continuity equation, the concentration distribution within a microfluidic chamber can be found,

$$\frac{\delta c}{\delta t} = -\nabla \cdot (-D \nabla c + c\mathbf{u}). \tag{3.8}$$

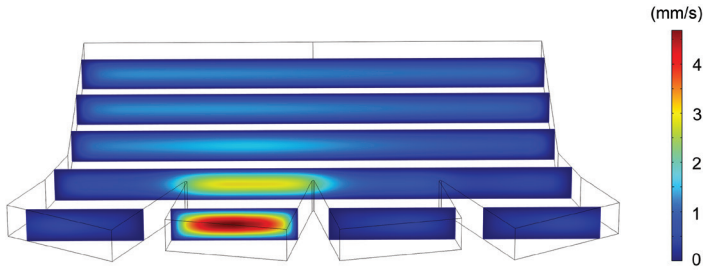


**Figure 3.2:** Simulation of the velocity profile in a microfluidic flow chamber with four inlet channels. The no-slip condition is clearly visible, with zero velocity at the channel walls and high velocity in the center of the channels. The flow used in the second channel from the left has an average flow velocity of 2.5 mm/s, but due to the no-slip condition the flow will reach a velocity greater than 4 mm/s in the center of the channel.

In the experiments in this work, all cells should be exposed to the same concentration of a solution, without concentration gradients. It is then essential that the cells are fully covered by the intended solution both before and after changes of flow rates. To know where the cells should be positioned the concentration distribution within the microfluidic chamber must be determined. In this work this was done through simulations using COMSOL Multiphysics® with the application modules *Incompressible Navier-Stokes* and *Convection-Diffusion*. In the *Incompressible Navier-Stokes* module, it was assumed that the fluid is Newtonian, that there are no body forces and that the walls of the chamber follow a no-slip condition. A more detailed description of the simulations can be found in **Paper I**, and below a few important aspects are highlighted.

Parameters that determine the concentration distribution and the velocity profile are the dimensions of the microfluidic chamber, the flow rates, and the concentration and the diffusion coefficient of the chemical in the fluid. Cyanide has a higher diffusion coefficient than e.g. glucose and this will lead to a broader concentration gradient and a smaller area where the cells can be positioned and still experience a homogeneous concentration.

Due to the no-slip condition, the flow speed is not constant throughout the entire cross-section of a channel. Along the walls of the channel, the velocity is lower than the average velocity and subsequently the velocity is higher than the average velocity in the center of the channel (Fig. 3.2). Since the cells are positioned at the bottom of the chamber, the flow velocity the cells experience will thus differ from the average flow velocity of the channel. Due to the lower flow velocity close to a channel wall, diffusion will there have longer time to participate in mass transport. To determine the largest concentration gradient due to diffusion, the analysis of the simulated results should be performed close to the channel wall where the cells are positioned.

The conformance between simulations and experimental measurements of the concentration distribution for flow velocities used in **Papers I-IV** can be seen in Fig. 3.3, where fluorescein was used in the experiments and a corresponding diffusion coefficient of $0.425{\cdot}10^{-9}$ $m^2/s$ was used in the simulations [77].

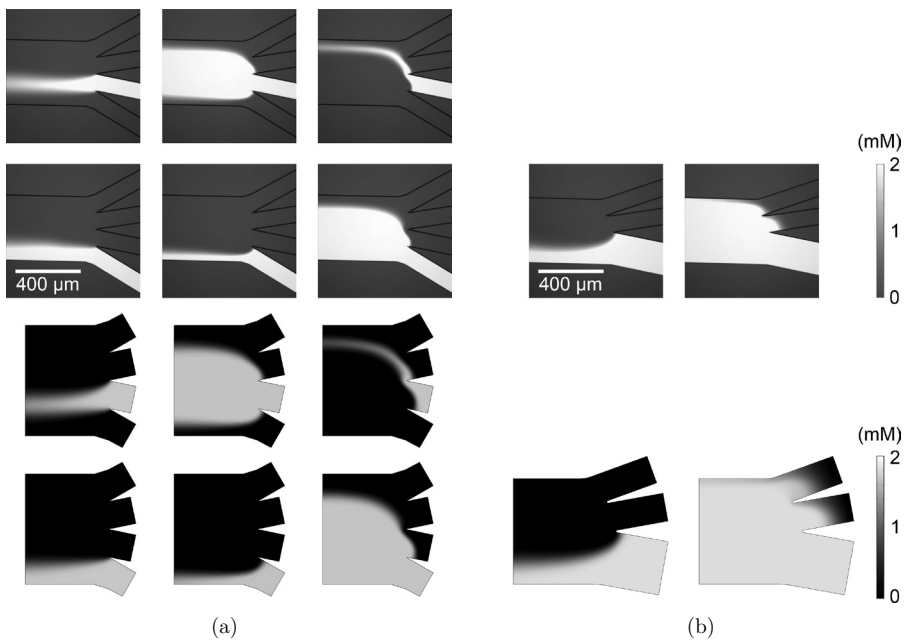


**Figure 3.3:** Image showing experimental measurements (top) and simulations (bottom) of the concentration distribution of fluorescein in a microfluidic flow chamber with (a) four inlet channels with flow rate settings as used in **Papers I**, **II** and **IV** and (b) three inlet channels with flow rate settings as used in **Paper III**.

### 3.1.4 Imaging of NADH fluorescence

Oscillations in glycolysis can be studied by imaging the autofluorescence from NADH molecules in the individual cells. To measure the fluorescence light from the NADH molecules a DAPI filter set was used, which corresponded well with the excitation and emission spectra of NADH (Fig. 3.4).

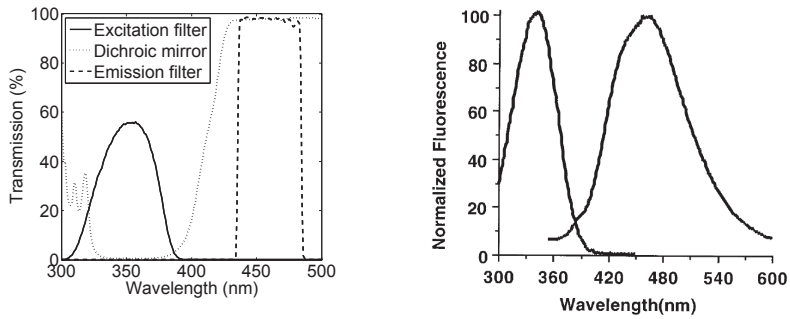


(a) (b)

**Figure 3.4:** (a) Spectra for the excitation filter, the dichroic mirror and the emission filter in a DAPI filter set (49000-ET-DAPI, Chroma). Data used by permission of Chroma Technology Corporation. (b) Excitation and emission spectra of the autofluorescent molecule NADH. The optimum excitation and emission wavelengths can be found at 340 nm and 465 nm respectively [78]. Copyright (2000) National Academy of Sciences, USA.

When exciting the NADH molecules, there is always a risk of photobleaching (Fig. 3.5). Bleaching of the molecules limits the total number of frames that can be acquired and thus limits either the temporal resolution or the total measurement time. It might also chemically harm the cells (see Section 3.1.2). In the experiments in this work, where an image was acquired every other or every fourth second and an intensity of 15 W (before the optics of the setup) and an exposure time of 200 ms was used, photobleaching has not been an issue. Even in measurements lasting up to one hour, no significant bleaching could be observed (Fig. 3.6(a)). However, care has to be taken regarding exposure time and intensity used, as can be seen in Fig. 3.6(b), where the intensity was increased to 30 W and the exposure time was set to 1000 ms. Here significant bleaching was observed and due to the strong illumination, the cell also lost its oscillatory behavior.

Another phenomenon that causes the fluorescence from molecules to decrease is called quenching. It differs from photobleaching in that the loss of fluorescence is only temporary. In quenching, the fluorescent molecule can collide with a non-fluorescent molecule and do a radiation-less relaxation to the ground state (collisional quenching) or the fluorescent molecule can form a non-fluorescent complex with another molecule (static quenching). In both cases, the fluorescence intensity from the cell is decreased. When measuring the fluorescence intensity while changing the environment, quenching can cause misinterpretations

since the fluorescence intensity rapidly decreases if the fluorescent molecule is quenched by a molecule in the new environment. However, no signs of quenching could be seen in the experiments in this work.

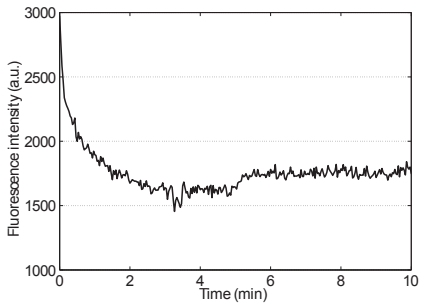


**Figure 3.5:** Graph showing the NADH autofluorescence from a cell. Capturing images every other second with an intensity of the excitation light of 30 W (before the optics of the setup) and an exposure time of 1000 ms caused significant photobleaching of the NADH molecules already within the first two minutes of the measurement.

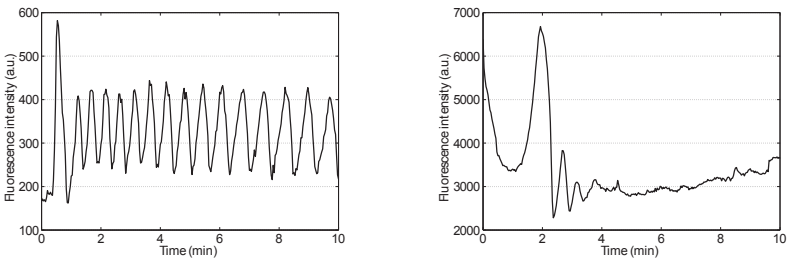


(a) (b)

**Figure 3.6:** (a) Graph showing the NADH autofluorescence from a cell performing sustained glycolytic oscillations. Images were captured every other second, the intensity of the excitation light was 15 W (before the optics of the setup) and the exposure time was 200 ms. (b) Cell exposed to the same environment as the cell in (a), but here the intensity of the light was increased to 30 W and the exposure time was 1000 ms. The NADH molecules were clearly photobleached during the first minutes of the measurement (compare to Fig. 3.5) and the strong illumination also caused the cell to lose its oscillations.

## 3.2 Data analysis

To investigate cell responses and characterize the oscillatory behavior of the cells, the images of the NADH fluorescence must be analyzed. Parameters that characterize the individual cell oscillations are e.g. frequency and amplitude and analysis of these parameters can reveal information about the mechanism giving rise to the oscillations. However, when investigating synchronization of several oscillators it is not sufficient to just analyze the frequency and amplitude, since oscillators can have the same amplitude and frequency without necessarily being synchronized. To investigate synchronization of oscillators, also their time-variant phases must be evaluated. The phases can then be used to quantify the degree of synchronization by the means of an order parameter. In this section the methods and procedures of data analysis used in **Papers I-IV** are described and the choices of specific parameters used in the analysis are discussed.

### 3.2.1 NADH time signal

To analyze the NADH autofluorescence from individual cells, images taken during the experiment were analyzed using the software ImageJ (http://imagej.nih.gov/ij/). A region of interest (ROI) was positioned around each cell, where the boundary of the ROI was positioned at the black cell boundary in the brightfield image taken at the start of the experiment. A brightfield image taken at the end of the experiment was used to see if the cells had moved during the experiment or if the focus had shifted. If a cell had moved slightly, the ROI was extended to ensure that the entire cell was within the ROI during the entire experiment. A ROI was also positioned outside of the cell array to measure the background intensity. The mean intensity from the background ROI was subtracted from the mean intensity of the cell ROIs at each time point to remove background noise and fluctuations. This analysis procedure was sufficient to determine whether cells were oscillatory or not. If also the amplitude of the oscillations was of interest, the measured amplitude was divided by the mean fluorescence signal after background subtraction (see also Section 3.2.3). If the cells drifted out of focus during the experiment, the amplitude of the oscillations would seem to decrease, but so would the mean of the signal. The same situation would occur if the cells moved slightly during the experiment. Then the ROI had to be extended, causing both the mean of the signal and the amplitude to decrease. Dividing the amplitude by the mean of the signal would then reduce the problems of both focus drift and moving cells.

### 3.2.2 Frequency

To analyze the frequency of the oscillations, the signal was Fourier transformed using MATLAB®. Since the period time of the oscillations in intact cells is around 30-60 s [3], corresponding to a maximum frequency of 0.033 Hz, the sampling frequency $f_s$ should exceed 0.066 Hz to resolve the fundamental frequency of the oscillations according to the sampling theorem. The sampling frequency of 0.25 Hz (0.5 Hz in **Papers III** and **IV**) used in this work was thus sufficient to resolve the fundamental frequency of the oscillations.

The frequency resolution obtained by the Fourier transform is

$$\Delta f = \frac{1}{T_{tot}} = \frac{f_s}{N}, \tag{3.9}$$

where $T_{tot}$ is the total time of the analysis interval and $N$ is the total number of samples in the interval [79]. To achieve higher resolution in the frequency analysis a long time interval should thus be used in the Fourier transform. However, since the frequency changed slightly during the measurements, the resolution decreases if a too long interval was used. Using an interval of around 5 min was empirically found to be a good compromise to minimize drift in frequency while still achieving high enough resolution.

The signal oscillated around a constant non-zero value, causing a peak in the amplitude spectrum at $f = 0$ Hz. To reduce the risk of losing the frequency component from the oscillations in the noise from the peak at $f = 0$ Hz, the mean of the signal was subtracted in the analysis interval before the Fourier transform was performed (in **Paper IV** the running average was used, see Section 3.2.4). The frequency was then evaluated using the `findpeaks` algorithm in MATLAB® to detect the highest peak in the single-sided amplitude spectrum.

### 3.2.3 Amplitude

To investigate the mechanism giving rise to oscillations in individual cells and to compare the oscillatory behavior of individual cells to population responses, the amplitude of the oscillations was analyzed in **Paper III**. Cells having a peak in the single-sided amplitude spectrum larger than 120 a.u. in time interval $\Delta t_2$ = 10-15 min were regarded as oscillatory. This peak height corresponded to oscillations detectable during manual analysis of the NADH time signal.

The amplitude of the oscillations from cells with a qualified peak were analyzed by

$$A_{\Delta t_i} = \frac{< A_{peak,\Delta t_i} > - < A_{valley,\Delta t_i} >}{2}, \tag{3.10}$$

where $< A_{peak,\Delta t_i} >$ and $< A_{valley,\Delta t_i} >$ corresponded to the average NADH time signal value of the peaks and valleys of the oscillations respectively in time intervals $\Delta t_i$ of 7-12 min, 10-15 min and 13-18 min for i = 1-3 respectively. The peaks and valleys of the oscillations were found using the `findpeaks` algorithm in MATLAB®. When the positions of the valleys were investigated, the signal was multiplied by $-1$ to facilitate use of `findpeaks`. The amplitudes were then normalized by dividing by the average NADH time signals in the corresponding time intervals.

The aim of the amplitude analysis was to find the amplitude of cells showing sustained oscillations. To discard cells showing transient oscillations (which thus could have a qualified peak in the amplitude spectrum, but a drastically changing amplitude in the analysis interval), the ratio of the amplitudes in time intervals 13-18 min and 7-12 min, $A_{ratio}$, was evaluated for each cell and was required to be within the range

$$0.5 < A_{ratio} = \frac{A_{\Delta t_3}}{A_{\Delta t_1}} < 2. \tag{3.11}$$

Cells fulfilling both the requirement of a qualified peak in the amplitude spectrum and the requirement for sustained oscillations were used in the analysis of the amplitude (and

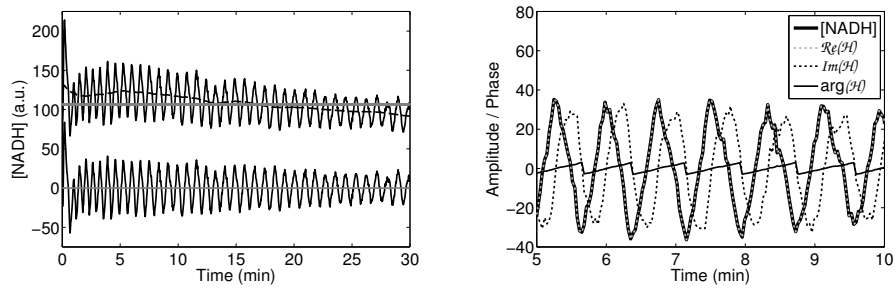


(a) (b)

**Figure 3.7:** (a) Graph showing the NADH fluorescence intensity from a single oscillating cell (top), where the straight grey line shows the total average of the signal and the dashed line shows the running average calculated with a window of approximately two periods. Below, the same signal after subtracting the running average is shown. After subtracting the running average, the signal oscillates around 0, which is a requirement for extraction of the instantaneous phase of the signal. (b) The running average corrected signal from (a), the real and imaginary parts of its Hilbert transform, and the instantaneous phase of the signal calculated as the argument of the Hilbert transform.

frequency) in time interval 10-15 min. A minimum of 10 qualified cells were required for evaluation of a concentration, otherwise the data set was discarded.

To compare our results with previous results from populations, the oscillation amplitude at each concentration was presented as the mean of the amplitudes of the individual cells multiplied by the fraction of cells that were oscillatory. In this way the "population equivalent" of the amplitude was achieved, without the additional requirement of synchronization.

### 3.2.4 Phase

To investigate the mechanism of synchronization, the phase responses of individual cells to periodic perturbations were analyzed in **Paper IV**. To facilitate extraction of the phases (and to further reduce the peak at $f = 0$ Hz in the amplitude spectrum) the running average of the NADH time signal was subtracted from the signal to reduce spurious drifts and trends (Fig. 3.7(a)).

To extract the instantaneous phases of the oscillations in individual cells, the running average-corrected time signals were Hilbert transformed [80] in MATLAB® using the `hilbert` algorithm. The transformed signal $\mathcal{H}$ was a complex analytical approximation of the original time signal, where the real part was equal to the original signal and the imaginary part was the Hilbert transform of the signal. The phases were then calculated as the argument of $\mathcal{H}$ (Fig. 3.7(b)).

Phase shifts were calculated as the difference in phases nine seconds after and before perturbations. The delay of nine seconds was chosen to give the cells long enough time to respond to the perturbations but short enough time to minimize effects from frequency

heterogeneity and drift. Corrected phase shifts were also calculated, where the expected phase shifts were subtracted from the initially calculated phase shifts. The expected phase shifts were calculated as the frequencies of the individual cells in the interval just before the perturbations multiplied by the time between the phase measurements before and after perturbations.

### 3.2.5 Order parameter

In **Paper IV**, the synchronization mechanism and its robustness to cell heterogeneity were investigated. For this to be possible, the order of the phases of the oscillations had to be quantified. Mathematically, synchronization between weakly coupled oscillators can be described using the Kuramoto model [81]. This is a paradigmatic model which in the mean field theory can be formulated in terms of an order parameter [51, 82],

$$re^{i\Psi} = \frac{1}{N}\sum_{j=1}^{N} e^{i\theta_j}, \tag{3.12}$$

where $r$ measures phase coherence, $\Psi$ is the average phase of all $N$ cells, and $\theta_j$ is the phase of cell $j$. The magnitude of the order parameter can then be found from

$$r = \left| \frac{1}{N}\sum_{j=1}^{N} e^{i\theta_j} \right|, \tag{3.13}$$

where $0 \leq r \leq 1$. Hence, $r$ gives a measure of the order of the phases of the oscillations, where a value close to unity indicates high degree of synchronization and a value close to zero indicates large heterogeneity in phases (Fig. 3.8). However, $r$ is expected to tend to zero for large heterogeneity only if $N$ is large. In general, $r$ is expected to be of the order of $1/\sqrt{N}$, assuming that the phases of individual cells are independent.

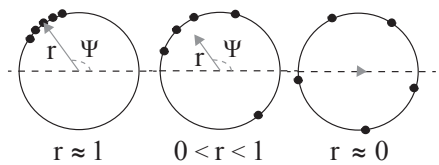


**Figure 3.8:** Schematic showing the dependence of the order parameter $r$ on the phases of the individual cells (here depicted as black dots on the unity circle), where $\Psi$ is the average phase of all cells. If all cells oscillate in phase (left) the order parameter is close to unity, while if there instead is large heterogeneity in phases (right), the order parameter is close to zero.

An example of quantification of the order of phases of the oscillations can be seen in Fig. 3.9, where ten individual cells initially were entrained by a periodic external perturbation, resulting in an order parameter close to unity. During the second half of

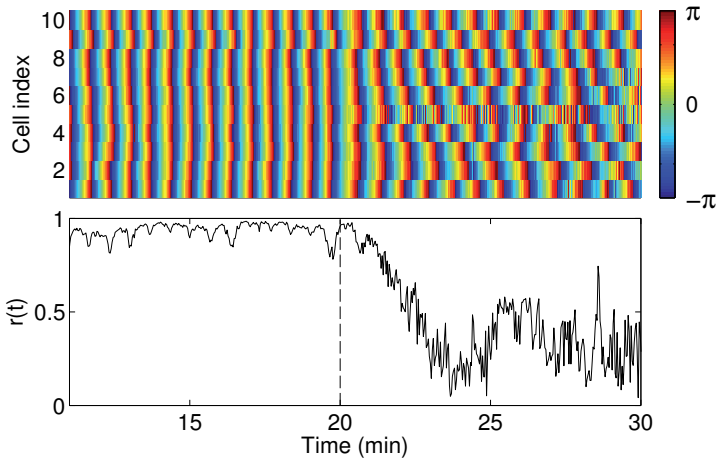


**Figure 3.9:** Graphs showing the instantaneous phases of oscillations from ten individual cells (top) and the order of the phases calculated using the Kuramoto order parameter described in Eq. 3.13 (bottom). The cells were entrained by a periodic perturbation in time interval 10-20 min, resulting in an order parameter close to unity. Without perturbations the order parameter decayed to a value of the order of $1/\sqrt{10}$. Data reproduced from Fig. 1 in **Paper IV**.

the measurement the cells were unperturbed. The lack of cell-cell interactions sustaining synchronization caused the order parameter to decay to a value of around $1/\sqrt{10}$.

## 3.3 Modeling the glycolytic reaction network

Studying a complex system such as glycolytic oscillations, it can be difficult to experimentally determine how different parts of the reaction network are related, how they give rise to collective behavior and how the system interacts with its environment. Here mathematical models can be of great use to describe a system and to make predictions of its behavior.

Many different models have been used to describe yeast glycolysis, from core models with few degrees of freedom that were used to illustrate a principle [18, 24, 83], to detailed kinetic models used for qualitative descriptions and predictions [9, 84–86]. In some cases, using core models instead of detailed models can be advantageous, e.g. for gaining fundamental understanding of the core mechanisms of a certain behavior. In this case the complexity of detailed models can cause difficulties in identifying the dominant mechanism responsible for the emergent behavior. The disadvantage with core models is that there is no direct mechanistic interpretation of the kinetic parameters; the values of the parameters are chosen so that the behavior of interest emerges. The drawback with previously constructed detailed kinetic models is that they are fitted to the data set of

interest to investigate whether the model can describe the data or to test a hypothesis. Those models are thus not thoroughly validated and rarely succeed in predicting results of other studies. For a model to be useful for investigation and prediction of behavior also in other studies, and to allow merging of different models as in a modular modeling approach [87], the parameters of the model should preferably be determined experimentally under physiological conditions. For detailed kinetic models describing yeast glycolysis, this means that enzyme kinetics data should be determined experimentally under conditions where the enzymes are active *in vivo*.

One such detailed kinetic model of yeast glycolysis is the du Preez model (Fig. 3.10) [88, 89], where the change in the concentration of a metabolite is described by the rate of the enzymes producing and consuming it. These reaction rates are modelled as a vector of functions $\mathbf{F}$, consisting of rate equations which depend on the concentrations $\mathbf{c}$ of different metabolites and the experimentally determined kinetic rate constants $\mathbf{p}$ of the involved enzymes. The reaction rates can then be written on a general form using ordinary differential equations,

$$\frac{d\mathbf{c}}{dt} = \mathbf{F}(\mathbf{c}, \mathbf{p}), \tag{3.14}$$

where

$$\mathbf{c} = \begin{pmatrix} c_1 \\ c_2 \\ c_3 \\ \vdots \end{pmatrix} \text{ and } \mathbf{p} = \begin{pmatrix} p_1 \\ p_2 \\ p_3 \\ \vdots \end{pmatrix}. \tag{3.15}$$

The rate equations must follow the law of mass action, which says that the rate is proportional to the product of the concentration of the involved reactants, each raised to a power depending on the number of the reactant molecules involved in the reaction [90]. The rate equations differ for the different enzymes and detailed knowledge about the enzymes is required to obtain an accurate description of the reactions.

Since intermediate metabolites can be products in one reaction step and substrates in the next reaction step, these equations describe a tree of reactions. However, reactions in different parts of this tree are connected through pools of shared reactants, such as NADH and ATP, resulting in the network of reactions depicted in Fig. 3.10.

In **Paper I**, the du Preez model was adapted to describe single cell oscillations within the microfluidic flow chamber, which included accounting for the removal of the secreted products ACA and ethanol by the flow in the chamber. Within the microfluidic flow chamber, the environment is not well stirred, as is assumed in the previous models [86, 88, 89]. The model thus had to be extended to explicitly describe the extracellular concentrations of ACA and ethanol, using the equation for diffusion through a membrane as a model for diffusion through a boundary layer surrounding each cell.

From the start, the model displayed accumulation of glucose 6-phosphate (G6P), fructose 6-phosphate (F6P) and fructose 1,6-bisphosphate (F16bP) [91]. This behavior was caused by the fast removal of ACA by the flow in the chamber and occurred also for the lowest possible flow rates used experimentally. This behavior was not observed experimentally and the model was adjusted to suppress this response by increasing the capacity of the glycerol branch to 300% and decreasing the ATPase activity to 20%.

There was heterogeneity in response from the individual cells at the change in flow rates (addition of cyanide), suggesting that the cells were close to a bifurcation point (transition between stable steady-state and oscillatory behavior). To position the bifurcation of the model between the two experimental regimes, the activity of the glucose transporter (GLT) was lowered to 80%.

Allowing for different initial concentrations of the metabolites, the vast majority (96.2%) of cell responses found experimentally could be simulated by allowing ±2% variations in the activity of the glucose transporter.

In **Paper III** it was shown that the NADH concentration in an oscillatory cell increases when the glucose concentration is decreased, in contrast to the behavior shown using the model in **Paper I**. To adapt the model to this experimentally shown behavior, the glycerol branch (which consumes NADH) was modified by increasing the sensitivity of the enzyme glycerol-3-phosphate dehydrogenase (G3PDH) to changes in the concentration of dihydroxyacetone (DHAP) (and glycerol 3-phosphate (G3P)) (Fig. 3.10). This adaptation also resulted in a qualitatively correct prediction of the frequency dependence on glucose.

The model was further improved by including the recently described cyanide reactions with pyruvate and DHAP, in addition to ACA [23]. This resulted in a qualitatively correct prediction of the two bifurcation points for cyanide titrations. To achieve a semi-quantitatively correct response, the binding constants of pyruvate and DHAP were increased by factor of 10. To obtain a model that did not oscillate without cyanide addition, the ACA diffusion rate was decreased by a factor of 4.

In **Paper IV**, the mechanism of synchronization was investigated. In contrast to the apparent robustness of this mechanism observed experimentally in dense cell cultures [3], synchronization appears to be much more difficult to achieve using mathematical models [9, 88, 92, 93].

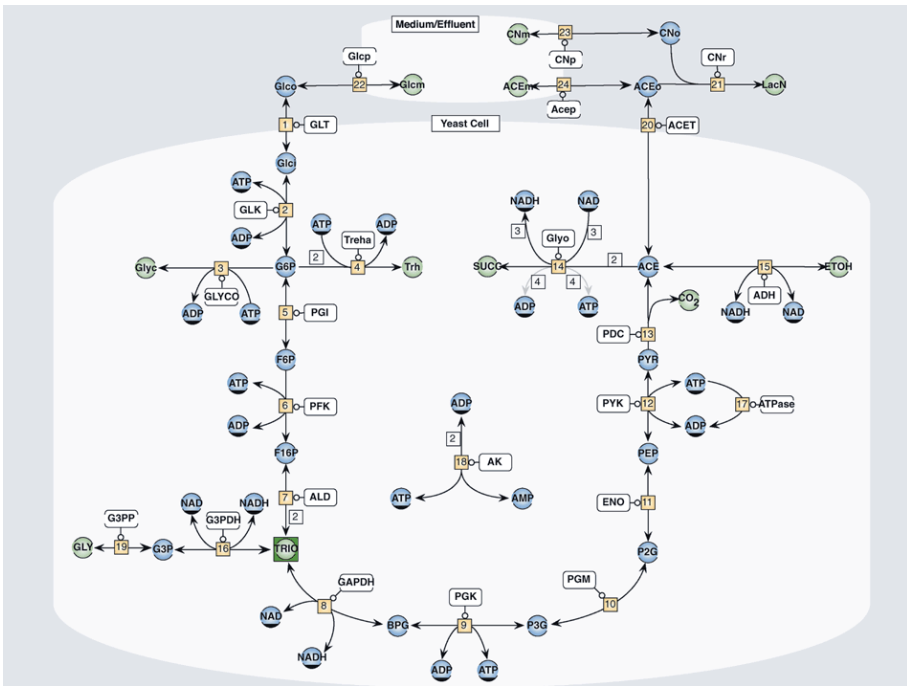


**Figure 3.10:** Schematic showing the reaction network of the du Preez model [88]. Intermediates (reactants and products) are indicated by circles, where green intermediates are so-called external variables, i.e. kept at constant concentration in the model. Circles with filled bottom parts mark intermediates that are shared between different parts of the network. Arrows represent reactions and their direction and white rectangles connected to a numbered square represent the enzyme catalyzing the reaction. The numbers in the squares represent the specific reaction steps in the network. Several arrows through a reaction step indicates that the reaction involves several intermediates. ACE, acetaldehyde; ACET, acetaldehyde transport; ADH, alcohol dehydrogenase; AK, adenylate kinase; ALD, fructose 1,6-bisphosphate aldolase; BPG, 1,3-bis-phosphoglycerate; CN, cyanide; ENO, phosphopyruvate hydratase; ETOH, ethanol; F16P, fructose 1,6-bisphosphate; F6P fructose 6-phosphate; GAPDH, D-glyceraldehyde-3-phosphate dehydrogenase; G3P, glycerol 3-phosphate; G3PDH, glycerol 3-phosphate dehydrogenase; G3PP, glycerol branch; G6P, glucose 6-phosphate; Glc, glucose; GLK, glucokinase; GLT, glucose transporter; GLY, glycerol; Glyc, glycogen; Glyco, glycogen branch; Glyo, succinate branch; LacN, lactonitrile; P2G, 2-phosphoglycerate; P3G, 3-phosphoglycerate; PEP, phosphoenolpyruvate; PDC, pyruvate decarboxylase; PGI, glucose-6-phosphate isomerase; PFK, 6-phosphofructokinase; PGK, phosphoglycerate kinase; PGM, phosphoglycerate mutase; PYK, pyruvate kinase; PYR, pyruvate; Treha, trehalose branch; TRIO, sum of glyceraldehyde 3-phosphate (GAP) and dihydroxyacetone phosphate (DHAP) (see also Fig. 1.1(a)); Trh, trehalose; SUCC, succinate branch. Figure reprinted from [88] by permission of John Wiley and Sons.

# Chapter 4

# Results and Discussion

## 4.1 Paper I: Induction of glycolytic oscillations in isolated cells

In **Paper I**, it was shown how glycolytic oscillations can be induced and studied on the single cell level by combining optical tweezers for cell positioning, microfluidics for environmental control and fluorescence microscopy for detection. It was shown that cells in isolation indeed can oscillate and that a high cell density is not a requirement for oscillations to emerge. My data revealed great heterogeneity in the response from the individual cells and four categories of cell behavior were identified. The first category constituted cells that showed sustained oscillations already when only glucose was added. The cells in the second and third category showed damped or no oscillations respectively for glucose and sustained oscillations only after cyanide addition. The cells in category four showed no oscillations at all. The results indicate that cells show a stronger tendency to oscillate when cyanide is present, but that oscillations also can be induced without cyanide within a flow chamber. The high flow rates in the chamber seem to, at least partially, be able to replace the role of cyanide for ACA removal.

A detailed kinetic model was also used to simulate the heterogeneous behavior of the cells and by allowing 2% difference in the glucose transporter activity, all four categories of oscillatory behavior were successfully simulated.

There can be several possible reasons to why previous attempts of studying single-cell oscillations have been inconclusive. In the study by Aon *et al.* it was shown that single cells within a dense population continued to oscillate out of phase also for some time after the macroscopic oscillations had died off [12]. This study did, however, not address whether a high cell density is required for induction of oscillations in the individual cells or if oscillations can be induced also in isolated cells. In a later study by de Monte *et al.*, oscillations could not be detected in single cells at low cell densities [45]. Hence, it was concluded that oscillations disappear synchronously in individual cells and in the population and that a high cell density is required for oscillations to be induced. This was explained by a dynamic quorum-sensing mechanism, where the oscillations are a collective property of the cells in the population. In their experiment, a well-stirred cuvette was used, where cells, glucose, and cyanide could be continuously flowed into the cuvette by pumps. The fluorescence was measured from cells in a thin layer near the surface of the

cuvette. With this setup, it should be possible to ensure oscillatory conditions for single cells. One reason why single cell oscillations were not detected could be that the detector was not sensitive enough to resolve oscillations from single cells. Another reason might be that the detector measured the average signal from many cells, which can average to a steady-state appearance if a significant distribution of oscillatory phases is present. In a study by Poulsen *et al.* [28], cells were immobilized in isolation on the bottom of a flow chamber, where the flow of chemicals were controlled by pumps. Individual cells were then imaged using an epi-fluorescence microscope and a light-sensitive camera. The experimental setup resembles that used in my work, but despite several attempts, the authors were not able to induce oscillations in isolated cells. It is difficult to address which differences in their experimental setup that may cause the cells to become non-oscillatory. The dimensions of the flow chamber are larger in the study by Poulsen compared to the chamber described in this work, which might have led to more turbulent flows and different flow rates. However, neither turbulent flow nor higher/lower flow rates should in principle prevent oscillations from emerging. Also in the work by Chandra *et al.* it is difficult to elucidate why no oscillations could be detected [46]. In a recent publication by Weber *et al.* [94], desynchronization with respect to cell density was investigated in the form of an order parameter (see Section 3.2.5). This study highlights the importance of understanding the heterogeneous behavior of individual cells and verifies that single cells can oscillate at low cell densities, without synchronization.

## 4.2 Paper II: Dependency of oscillatory behavior on flow rates

When using microfluidics to control the extracellular environment, the chemicals in the solutions rather than the flow rates should determine the behavior of the cells. The role of flow rates on the oscillatory behavior of individual yeast cells was investigated in **Paper II**.

At the beginning of the experiment, cells were exposed to either glucose or to both glucose and cyanide at the same flow rate settings. The flow rates were then changed and all cells were exposed to both glucose and cyanide. Cells only exposed to glucose at the beginning of the experiment thus experienced a change in both chemicals and flow rates, while cells that were exposed to both glucose and cyanide already from the beginning only experienced a change in flow rates. In the latter case oscillations were induced in most cells at the start of the experiment and no response could be seen at the change in flow rates. However, in cells exposed to only glucose at the beginning of the experiment, sustained oscillations were in most cells induced first at the flow rate change, were the cells also were exposed to cyanide.

These experiments clearly indicate that the chemicals in the solutions rather than the flow rates determine the oscillatory behavior of the cells, at least in the range of flow rates used in this work. This verification facilitate quantitative investigation of how cell responses depend on the concentrations of glucose and cyanide.

## 4.3 Paper III: Mechanism and conditions for oscillations in individual cells

In **Paper III** it was found that the conditions required for oscillations to emerge in individual cells are qualitatively similar to the conditions required for synchronized oscillations to be detected in populations [9]. However, the range of conditions inducing oscillations in individual cells was much wider when there was no additional requirement of synchronization. This shows that the conditions required for synchronized oscillations is a subset of the conditions required for oscillations in individual cells, and indicates that individual cells might be oscillating also in an apparent non-oscillatory population. This supports the viewpoint that coherence in population oscillations results from synchronization of individual oscillators via a Kuramoto transition (see also **Paper IV**) [81].

Similar frequency dependence on glucose concentration was observed as had previously been detected in population studies [9, 10]. However, this dependency was found to increase drastically for very low glucose concentrations, where no oscillations are detected in populations. The frequency distribution among the cells also became broader at these low glucose concentrations. The broadening of the frequency distributions might be the answer to why no synchronized oscillations are detected in this glucose range. If synchronization can be described as a Kuramoto transition, the propensity of the cells to synchronize will not only depend on the coupling strength between the cells, but also on the difference in frequency/phase. If the frequency distribution becomes too broad, it might then prevent the cells from synchronizing.

After a few adjustments of the detailed kinetic model used in **Paper I** (see Section 3.3) the model was able to semi-quantitatively predict both the concentrations of glucose and cyanide required for oscillations to emerge and the frequency response to changes in glucose and cyanide concentrations.

Having determined the precise conditions for induction of oscillations in individual cells, an attempt was made to relate these conditions back to the mechanism responsible for glycolytic oscillations. Two mechanisms have been suggested; (i) phosphofructokinase (PFK) has been suggested as oscillophore [95] (i.e. the master enzyme controlling the oscillations) on the basis of its kinetic mechanism [24, 83], where oscillations are assumed to be induced by instabilities caused by substrate (ATP) inhibition and product (AMP) activation of the enzyme. (ii) The autocatalytic stoichiometry of the glycolytic pathway (ATP being substrate in the first part and product in the last part of the pathway) has been suggested as a positive feedback leading to oscillations [96].

To investigate the mechanism controlling the oscillations, the dimensionality of the model was reduced as shown in a previous study [97]. Despite the high dimensionality of the model, the onset and frequency of the oscillations could be interpreted in terms of positioning in a single, continuous state-space spanned by ATP, F6P and F16bP. Simulation of the cyanide titration caused transversal movement through the state-space, leading to the two bifurcation points, whereas glucose titrations caused longitudinal movement with a single bifurcation point and strong effect on the frequency. The chosen three variables gave the most well-defined boundary between oscillatory and stable steady-states. That the boundary was not exact, but had a small overlap between the states, indicated that some of the other parameters made a small contribution to the bifurcation points.

State-spaces for kinases different than PFK (glucokinase (GLK), phosphoglycerate kinase (PGK) and pyruvate kinase (PYK)) lacked well-defined boundaries.

ATP, F6P and F16bP are all effectors of the PFK. To test the hypothesis that allosteric regulation of PFK by ATP and AMP causes the oscillations, the elasticity [98] of PFK for ATP and AMP was analyzed in the state-space. The results showed that oscillations only occur within specific allosteric control values, indicating that the oscillatory behavior is determined by allosteric control of PFK. This is in agreement with the suggested role of PFK as oscillophore.

To further elucidate the suggested role of PFK as oscillophore, a control analysis [99] was performed. It showed that PFK did not have high control coefficient for the position of the bifurcation points or the frequency of the oscillations. However, the emergence of oscillations could always be related to PFK kinetics. This lead us to look for an extension of the definition of oscillophore, from being the controller of oscillations [95] to being the enabler of oscillations, without which oscillations could not occur. Rather than having large control of e.g. amplitude and frequency, PFK would then be a necessary condition for oscillations, while the rest of the system could provide the sufficient conditions.

To investigate whether also the stoichiometry could work as oscillophore within this new definition, the autocatalytic stoichiometry for ATP was reduced. This removed the oscillations, but these could be rescued by a reduction in the ATPase activity. Making small changes in the allosteric binding constants of PFK for ATP and AMP, however, eliminated the oscillations, which could not be rescued by perturbations in any other parts of the system.

This study thus suggests that allosteric regulation of PFK activity is the key kinetic component without which no oscillations can be observed. This makes PFK the oscillophore in terms of the necessary kinetic component - an oscillation enabler.

## 4.4 Paper IV: Mechanism of synchronization and its robustness and universality

To determine the mechanism of synchronization, how robust it is with regard to cell heterogeneity, and how universal it is with regard to different chemical species, the phase, frequency and amplitude responses of single-cell oscillations to periodic external perturbations were investigated in **Paper IV**.

The study showed that periodic addition of ACA caused entrainment of the individual cell oscillations, in agreement with previous population studies [16, 19]. Strikingly, it was also found that removal of cyanide caused similar entrainment, in contrast to previous studies [17]. Analyzing the phase of the oscillations, it could be seen that perturbations induced phase shifts, which depended on the phase of the oscillations when they were perturbed. The strongest response was achieved when the NADH concentration was at a minimum, where removal of cyanide prolonged the period by roughly one third. In contrast to model calculations [9], no entrainment in anti-phase was observed. The frequencies seemed largely unaffected by the perturbations, when compared in the interval before and after the perturbations. Also the amplitudes of oscillatory cells remained relatively constant. Calculating the phase shifts for several consequent perturbations, it was found that

entrainment occurred rapidly, already during the first few perturbations. This would result in fast cell-cell synchronization, which indeed has been observed experimentally when two populations oscillating 180° out-of-phase are mixed [16, 27]. These results indicate that oscillatory cells synchronize through phase shifts. However, also non-oscillatory cells became entrained by the perturbations. For this response to be detectable also the amplitude must become affected, indicating that phase changes alone are not sufficient to entrain non-oscillatory cells.

The degree of synchronization was determined using the Kuramoto order parameter (see Section 3.2.5). The order parameter increased rapidly in the perturbation interval, in agreement with the temporal phase shift analysis described above. Despite initially large heterogeneity in frequency and phase among the individual cells, the order parameter reached a value close to unity in the perturbation interval, indicating a high degree of synchronization. This showed that the synchronization mechanism is robust with regard to cell heterogeneity.

It has been shown that the phase dependence of the phase shift differs for different chemical species [19]. This study revealed that the phase response at cyanide removal resembles that of ACA addition, indicating that removal of cyanide causes entrainment through similar mechanism as ACA addition. The fact that different chemicals appear to synchronize oscillations through similar mechanisms indicates that the synchronization mechanism may be universal.

Using a flow chamber, ACA will be removed by the flow and anaerobic environment can be achieved by gassing the sample with an inert gas, as in a study by Poulsen *et al.* where argon was used [22]. In that study KOH was also added instead of KCN to adjust pH to facilitate oscillations. To investigate the biochemical mechanism through which cyanide removal can cause synchronization, entrainment was studied for perturbations with hypoxic glucose solutions and with pH-corrected hypoxic glucose solutions. In both cases entrainment could be seen, indicating that entrainment is caused by other effects of cyanide removal than activation of respiration or changes in pH. That cyanide can act in more ways than by binding ACA and inhibit respiration has been indicated in previous studies, where the oscillatory tendency was stronger when cyanide was added than under hypoxic conditions [15] and under hypoxic conditions where ACA was flushed away by a flow (**Paper I**). And indeed, recently Hald *et al.* showed that cyanide also reacts with other metabolites, namely pyruvate and DHAP, and that cyanide might affect the behavior of glycolytic oscillations in more ways than just by binding ACA and inhibiting respiration [23]. Previous studies have also shown that cyanide causes longer trains of oscillations than other inhibitors of respiration, such as antimycin A and azide [27, 100], and that oscillations disappear if both cyanide and azide are present [22]. The role of cyanide inhibiting respiration by binding to cytochrome *c* oxidase and the contribution of respiratory reactions to the oscillatory behavior have recently been discussed by Schrøder *et al.*, who found that oscillations disappear for strains with deletions of a gene coding for subunit VI of cytochrome *c* oxidase [101]. This finding was unexpected, since the general assumption is that cytochrome *c* oxidase is completely inhibited at cyanide concentrations used for oscillation studies and should not contribute at all to the oscillatory behavior of the cells [15]. Cyanide reactions with glucose have, however, been shown to be negligible in the pH range of our experiments [23]. Further studies are thus needed to elucidate the precise effect of the intracellular cyanide reactions.

# Chapter 5

# Conclusions and Outlook

In this work, it was shown how glycolytic oscillations can be induced and studied in individual, isolated yeast cells by combining optical tweezers for cell positioning, microfluidics for environmental control and fluorescence microscopy for detection. It was proven that single cells in isolation indeed can show sustained glycolytic oscillations and that a synchronized, high density cell culture is not a requirement for oscillations to emerge. These results are a milestone in the research about glycolytic oscillations and opens up for exciting studies of glycolysis on the single-cell level.

Having verified that the chemicals in the solutions determine the oscillatory behavior rather than the flow rates in the microfluidic flow chamber, the precise conditions required for oscillations to emerge in individual cells were determined. The results showed that individual cells can continue to oscillate at conditions where no synchronized oscillations are detected in populations. The detected increase in frequency distribution at low glucose concentrations might provide the answer to why cells do not synchronize at these conditions. Evaluating the conditions required for oscillations to emerge indicated that the mechanism behind oscillations in individual cells is allosteric regulation of the enzyme PFK.

Knowing the precise conditions required for oscillations to emerge in individual cells, the mechanism of synchronization and how it is affected by the found heterogeneity in cell response was determined. The results showed that oscillatory cells synchronize through phase shift and that this mechanism is robust with regard to cell heterogeneity. That different chemical species appear to synchronize cells through similar mechanisms indicates that such a mechanism can be at work also in other cell types, possibly via different metabolic species.

As a next step, the cell density in the array can be varied using the optical tweezers and cell-to-cell coupling and synchronization can be studied. That the cell density is important has been verified in several different studies in bulk (e.g. [11, 12, 45]), and recently also in single-cell studies [94]. The flow in the microfluidic chamber can be used as an advantage, where a cell can be positioned at different distances downstream of another cell and possible influence on the cell downstream from ACA secreted from the cell upstream can be investigated. However, the flow might be an issue for synchronization studies if the secreted ACA is washed away too rapidly. In the microfluidic chamber, the lowest flow rate that should be used is limited by the requirement for complete coverage of the entire array with the intended solution. If high flow rates turn out to be an issue,

fabricating microfluidic systems with valves, where all flows can be turned off, might be a solution. The flexibility in the choice of microfluidic flow chamber design and flow rates makes microfluidics very useful for these types of studies.

To gain more detailed knowledge about the reaction network, several different metabolites should be measured simultaneously. This would reveal e.g. in what part of the network a stimulus is registered and if there is a delay in the transfer of the response to other parts of the network. One example is cell coupling via ACA. Since ACA is involved in the final branch of yeast glycolysis, it would be very interesting to investigate how strongly and how fast other parts of glycolysis are affected by changes in extracellular ACA concentration. One way to achieve this could be to use ATP probes [102]. Another way could be to measure the activity of pyruvate kinase, using a recently developed FRET-based pyruvate kinase activity reporter (PKAR) [33].

One unsolved question that remains to be answered is why cells oscillate. Are there any benefits of oscillations over steady-state with respect to speed or efficiency of glycolysis? Pye reported slower ethanol production after oscillations had died off, suggesting that oscillatory glycolysis is faster than steady-state [103]. It has also been suggested that oscillatory glycolysis yields more chemical energy such as ATP and less dissipation of heat [104]. However, experimental evidence is lacking. Perhaps glycolytic oscillations are just the result of the autocatalytic nature of glycolysis and have not been eliminated during evolution because they are not unfavorable for the cells.

The results presented in this work have advanced our understanding of the complex set of reactions in energy metabolism and the mechanisms through which cells oscillate, communicate, and synchronize. Pursuing these studies will hopefully not only give further information about glycolysis in yeast, but also about energy metabolism, oscillations, and communication in other biological systems, such as oscillatory insulin secretion from islets of $\beta$-cells.

# Acknowledgements

First and foremost, I would like to thank my supervisor **Dr. Mattias Goksör** for welcoming me to the group, for introducing me to the field of biophotonics, for always encouraging me to become a better researcher, and for helping me push my limits.

Special thanks also to my co-supervisor **Dr. Caroline Beck Adiels**, for your endless support and for always making time to discuss large and small issues.

Thanks also to my former and current room-mates **Dr. Martin Persson** and **Ricardo Silva** for your support and for patiently letting me turn our office into a greenhouse.

I also want to thank both former and current members of the Biophotonics group, **Dr. Kristin Sott**, **Dr. Anna Björnson Granqvist**, **Dr. David Engström**, **Amin Abbaszadeh Banaeiyan**, **Dr. Doryaneh Ahmadpour** and **Dr. Jonas Danielson** for making it a stimulating work environment and for making it fun to come to work.

My greatest gratitude also to my examiner **Prof. Bernhard Mehlig**, who has provided invaluable advice about this research project and about the art of scientific writing.

Thanks also to my mentor **Prof. Sheila Galt**. I really appreciate our lunch-discussions and find them both helpful and encouraging.

I also want to thank **Prof. Jacky Snoep**, **Dr. David van Niekerk** and **Dr. Franco du Preez** for letting me come to their group at the Stellenbosch University to learn about the complexity of detailed kinetic modeling. Thanks also to the other members of the group and all who took great care of me during my stay, and to **Dr. Bob Kooi** at the VU University in Amsterdam.

My gratitude also goes to **Dr. Lars Bengtsson**, for always being supportive and for answering my large and small questions about how to get the instruments in the lab to work and how to handle my data.

Thanks also to my friends for not forgetting me despite spending long days at work and special thanks to **Charlotte Hamngren Blomqvist** for making my undergraduate studies a lot of fun, for getting me started in the lab and for our lunch and tea breaks when they were needed the most.

Last but not least, my warmest thanks to my family: my parents **Ulla-Britt** and **Jan-Olof** and my brother **Daniel** for your endless support and for always showing interest in my work, and to my fiancé **Emil**, thank you for letting me be me, for knowing when not to argue about my long days at work (but also when to make me come home) and for supporting me throughout my PhD studies. "Just make it happen!" ;)

Göteborg, December 1, 2014
Anna-Karin Gustavsson

# References


[1] C. E. Cooper and G. C. Brown, The inhibition of mitochondrial cytochrome oxidase by the gases carbon monoxide, nitric oxide, hydrogen cyanide and hydrogen sulfide: chemical mechanism and physiological significance, *Journal of Bioenergetics and Biomembranes* **40**, 533–539 (2008).

[2] J. T. Pronk, H. Y. Steensma, and J. P. van Dijken, Pyruvate Metabolism in *Saccharomyces cerevisiae*, *Yeast* **12**, 1607–1633 (1996).

[3] P. Richard, The rhythm of yeast, *FEMS Microbiology Reviews* **27**, 547–557 (2003).

[4] L. N. M. Duysens and J. Amesz, Fluorescence spectrophotometry of reduced phosphopyridine nucleotide in intact cells in the near-ultraviolet and visible region, *Biochimica et Biophysica Acta* **24**, 19–26 (1957).

[5] B. Chance, R. W. Estabrook, and A. Ghosh, Damped sinusiodal oscillations of cytoplasmic reduced pyridine nucleotide in yeast cells, *Proceedings of the National Academy of Sciences of the United States of America* **51**, 1244–1251 (1964).

[6] A. Ghosh and B. Chance, Oscillations of glycolytic intermediates in yeast cells, *Biochemical and Biophysical Research Communications* **16**, 174–181 (1964).

[7] B. Hess, A. Boiteux, and J. Krüger, Cooperation of glycolytic enzymes, *Advances in Enzyme Regulation* **7**, 149–167 (1969).

[8] L. von Klitzing and A. Betz, Metabolic control in flow systems, *Archives of Microbiology* **71**, 220–225 (1970).

[9] F. Hynne, S. Danø, and P. G. Sørensen, Full-scale model of glycolysis in Saccharomyces cerevisiae, *Biophysical Chemistry* **94**, 121–163 (2001).

[10] K. A. Reijenga, J. L. Snoep, J. A. Diderich, H. W. van Verseveld, H. V. Westerhoff, and B. Teusink, Control of glycolytic dynamics by hexose transport in *Saccharomyces cerevisiae*, *Biophysical Journal* **80**, 626–634 (2001).

[11] J. Aldridge and E. K. Pye, Cell density dependence of oscillatory metabolism, *Nature* **259**, 670–671 (1976).

[12] M. A. Aon, S. Cortassa, H. V. Westerhoff, and K. van Dam, Synchrony and mutual stimulation of yeast cells during fast glycolytic oscillations, *Journal of General Microbiology* **138**, 2219–2227 (1992).

[13] P. Richard, B. Teusink, H. V. Westerhoff, and K. van Dam, *Synchronization of glycolytic oscillations in intact yeast cells*, In: *Modern Trends in Biothermokinetics*, (S. Schuster, M. Rigoulet, R. Ouhabi, and J. -P. Mazat, Eds.), Plenum Press, New York, USA (1993).

[14] P. Richard, B. Teusink, H. V. Westerhoff, and K. van Dam, Around the growth phase transition *S. cerevisiae*'s make-up favours sustained oscillations of intracellular metabolites, *FEBS Letters* **318**, 80–82 (1993).

[15] P. Richard, J. A. Diderich, B. M. Bakker, B. Teusink, K. van Dam, and H. V. Westerhoff, Yeast cells with a specific cellular make-up and an environment that removes acetaldehyde are prone to sustained glycolytic oscillations, *FEBS Letters* **341**, 223–226 (1994).

[16] P. Richard, B. M. Bakker, B. Teusink, K. van Dam, and H. V. Westerhoff, Acetaldehyde mediates the synchronization of sustained glycolytic oscillations in populations of yeast cells, *European Journal of Biochemistry* **235**, 238–241 (1996).

[17] S. Danø, P. G. Sørensen, and F. Hynne, Sustained oscillations in living cells, *Nature* **402**, 320–322 (1999).

[18] M. Bier, B. M. Bakker, and H. V. Westerhoff, How Yeast Cells Synchronize their Glycolytic Oscillations: A Perturbation Analytic Treatment, *Biophysical Journal* **78**, 1087–1093 (2000).

[19] S. Danø, F. Hynne, S. De Monte, F. D'Ovidio, P. G. Sørensen, and H. Westerhoff, Synchronization of glycolytic oscillations in a yeast cell population, *Faraday Discussions* **120**, 261–276 (2001).

[20] S. Danø, M. F. Madsen, and P. G. Sørensen, Quantitative characterization of cell synchronization in yeast, *Proceedings of the National Academy of Sciences of the United States of America* **104**, 12732–12736 (2007).

[21] A. Kloster and L. F. Olsen, Oscillations in glycolysis in *Saccharomyces cerevisiae*: The role of autocatalysis and intracellular ATPase activity, *Biophysical Chemistry* **165-166**, 39–47 (2012).

[22] A. K. Poulsen, F. R. Lauritsen, and L. F. Olsen, Sustained glycolytic oscillations – no need for cyanide, *FEMS Microbiology Letters* **236**, 261–266 (2004).

[23] B. O. Hald, M. Smrcinova, and P. G. Sørensen, Influence of cyanide on diauxic oscillations in yeast, *FEBS Journal* **279**, 4410–4420 (2012).

[24] A. Boiteux, A. Goldbeter, and B. Hess, Control of oscillating glycolysis of yeast by stochastic, periodic, and steady source of substrate: A model and experimental study, *Proceedings of the National Academy of Sciences of the United States of America* **72**, 3829–3833 (1975).

[25] M. Markus, D. Kuschmitz, and B. Hess, Chaotic dynamics in yeast glycolysis under periodic substrate input flux, *FEBS Letters* **172**, 235–238 (1984).

[26] A. T. Winfree, Oscillatory Glycolysis in Yeast: The Pattern of Phase Resetting by Oxygen, *Archives of Biochemistry and Biophysics* **149**, 388–401 (1972).

[27] A. K. Ghosh, B. Chance, and E. K. Pye, Metabolic Coupling and Synchronization of NADH Oscillations in Yeast Cell Populations, *Archives of Biochemistry and Biophysics* **145**, 319–331 (1971).

[28] A. K. Poulsen, M. Østergaard Petersen, and L. F. Olsen, Single cell studies and simulation of cell-cell interactions using oscillating glycolysis in yeast cells, *Biophysical Chemistry* **125**, 275–280 (2007).

[29] K. Tornheim and J. M. Lowenstein, The purine nucleotide cycle. III. Oscillations in metabolite concentrations during the operation of the cycle in muscle extracts, *Journal of Biological Chemistry* **248**, 2670–2677 (1973).

[30] K. Tornheim and J. M. Lowenstein, The purine nucleotide cycle. IV. Interactions with oscillations of the glycolytic pathway in muscle extracts, *Journal of Biological Chemistry* **249**, 3241–3247 (1974).

[31] R. Frenkel, Control of Reduced Diphosphopyridine Nucleotide Oscillations in Beef Heart Extracts, *Archives of Biochemistry and Biophysics* **125**, 157–165 (1968).

[32] K. H. Ibsen and K. W. Schiller, Oscillations of nucleotides and glycolytic intermediates in aerobic suspensions of Ehrlich ascites tumor cells, *Biochimica et Biophysica Acta* **131**, 405–407 (1967).

[33] M. J. Merrins, A. R. van Dyke, A. K. Mapp, M. A. Rizzo, and L. S. Satin, Direct Measurements of Oscillatory Glycolysis in Pancreatic Islet $\beta$-Cells Using Novel Fluorescence Resonance Energy Transfer (FRET) Biosensors for Pyruvate Kinase M2 Activity, *Journal of Biological Chemistry* **288**, 33312–33322 (2013).

[34] K. Tornheim, Are Metabolic Oscillations Responsible for Normal Oscillatory Insulin Secretion?, *Diabetes* **46**, 1375–1380 (1997).

[35] R. Bertram, A. Sherman, and L. S. Satin, Metabolic and electrical oscillations: partners in controlling pulsatile insulin secretion, *American Journal of Physiology - Endocrinology and Metabolism* **293**, E890–E900 (2007).

[36] D. L. Cook and C. N. Hales, Intracellular ATP directly blocks $K^+$ channels in pancreatic B-cells, *Nature* **311**, 271–273 (1984).

[37] T. Nilsson, V. Schultz, P. O. Berggren, B. E. Corkey, and K. Tornheim, Temporal patterns of changes in ATP/ADP ratio, glucose 6-phosphate and cytoplasmic free $Ca^{2+}$ in glucose-stimulated pancreatic $\beta$-cells, *Biochemical Journal* **314**, 91–94 (1996).

[38] D. R. Matthews, B. A. Naylor, R. G. Jones, G. M. Ward, and R. C. Turner, Pulsatile Insulin Has Greater Hypoglycemic Effect Than Continuous Delivery, *Diabetes* **32**, 617–621 (1983).

[39] G. Paolisso, A. J. Scheen, D. Giugliano, S. Sgambato, A. Albert, M. Varricchio, F. D'Onofrio, and P. J. Lefébvre, Pulsatile Insulin Delivery has Greater Metabolic Effects than Continuous Hormone Administration in Man: Importance of Pulse Frequency, *The Journal of Clinical Endocrinology and Metabolism* **72**, 607–615 (1991).

[40] D. A. Lang, D. R. Matthews, M. Burnett, and R. C. Turner, Brief, Irregular Oscillations of Basal Plasma Insulin and Glucose Concentrations in Diabetic Man, *Diabetes* **30**, 435–439 (1981).

[41] B. Fendler, M. Zhang, L. Satin, and R. Bertram, Synchronization of Pancreatic Islet Oscillations by Intrapancreatic Ganglia: A Modeling Study, *Biophysical Journal* **97**, 722–729 (2009).

[42] N. Pørksen, M. Hollingdal, C. Juhl, P. Butler, J. D. Veldhuis, and O. Schmitz, Pulsatile Insulin Secretion: Detection, Regulation, and Role in Diabetes, *Diabetes* **51**, S245–S254 (2002).

[43] O. Schmitz, J. Rungby, L. Edge, and C. B. Juhl, On high-frequency insulin oscillations, *Ageing Research Reviews* **7**, 301–305 (2008).

[44] M. Ristow, H. Carlqvist, J. Hebinck, M. Vorgerd, W. Krone, A. Pfeiffer, D. Müller-Wieland, and C. G. Ostenson, Deficiency of phosphofructo-1-kinase/muscle subtype in humans is associated with impairment of insulin secretory oscillations, *Diabetes* **57**, 1557–1561 (1999).

[45] S. De Monte, F. D'Ovidio, S. Danø, and P. G. Sørensen, Dynamical quorum sensing: Population density encoded in cellular dynamics, *Proceedings of the National Academy of Sciences of the United States of America* **104**, 18377–18381 (2007).

[46] F. A. Chandra, G. Buzi, and J. C. Doyle, Glycolytic oscillations and limits on robust efficiency, *Science* **333**, 187–192 (2011).

[47] A. K. Gustavsson, D. D. van Niekerk, C. B. Adiels, F. B. du Preez, M. Goksör, and J. L. Snoep, Sustained glycolytic oscillations in individual isolated yeast cells, *FEBS Journal* **279**, 2837–2847 (2012).

[48] A. K. Gustavsson, C. B. Adiels, and M. Goksör, Induction of sustained glycolytic oscillations in single yeast cells using microfluidics and optical tweezers, *Proceedings of SPIE* **8458**, 84580Y–1 – 84580Y–7 (2012).

[49] A. K. Gustavsson, D. D. van Niekerk, C. B. Adiels, B. Kooi, M. Goksör, and J. L. Snoep, Allosteric regulation of phosphofructokinase controls the emergence of glycolytic oscillations in isolated yeast cells, *FEBS Journal* **281**, 2784–2793 (2014).

[50] A. K. Gustavsson, D. D. van Niekerk, C. B. Adiels, M. Goksör, and J. L. Snoep, Heterogeneity of glycolytic oscillatory behaviour in individual yeast cells, *FEBS Letters* **588**, 3–7 (2014).

[51] S. Shinomoto and Y. Kuramoto, Phase Transitions in Active Rotator Systems, *Progress of Theoretical Physics* **75**, 1105–1110 (1986).

[52] H. Serizawa, T. Amemiya, and K. Itoh, Glycolytic synchronization in yeast cells via ATP and other metabolites: mathematical analyses by two-dimensional reaction-diffusion models, *Natural Science* **6**, 719–732 (2014).

[53] A. Ashkin, Acceleration and Trapping of Particles by Radiation Pressure, *Physical Review Letters* **24**, 156–159 (1970).

[54] A. Ashkin and J. M. Dziedzic, Optical Levitation by Radiation Pressure, *Applied Physics Letters* **19**, 283–285 (1971).

[55] A. Ashkin, J. M. Dziedzic, J. E. Bjorkholm, and S. Chu, Observation of a single-beam gradient force optical trap for dielectric particles, *Optics Letters* **11**, 288–290 (1986).

[56] A. Ashkin and J. M. Dziedzic, Optical Trapping and Manipulation of Viruses and Bacteria, *Science* **235**, 1517–1520 (1987).

[57] A. Ashkin, J. M. Dziedzic, and T. Yamane, Optical Trapping and Manipulation of Single Cells Using Infrared Laser Beams, *Nature* **330**, 769–771 (1987).

[58] J. El-Ali, P. K. Sorger, and K. F. Jensen, Cells on chips, *Nature* **442**, 403–411 (2006).

[59] D. C. Duffy, J. C. McDonald, O. J. A. Schueller, and G. M. Whitesides, Rapid Prototyping of Microfluidic Systems in Poly(dimethylsiloxane), *Analytical Chemistry* **70**, 4974–4984 (1998).

[60] J. C. McDonald, D. C. Duffy, J. R. Anderson, D. T. Chiu, H. Wu, O. J. A. Schueller, and G. M. Whitesides, Fabrication of microfluidic systems in poly(dimethylsiloxane), *Electrophoresis* **21**, 27–40 (2000).

[61] K. Sott, E. Eriksson, and M. Goksör, *Acquisition of Single Cell Data in an Optical Microscope*, In: *Lab on a Chip Technology: Biomolecular Separation and Analysis*, (K. E. Herold and A. Rasooly, Eds.), Caister Academic Press, Norfolk, United Kingdom (2009).

[62] E. Fällman and O. Axner, Design for fully steerable dual-trap optical tweezers, *Applied Optics* **36**, 2107–2113 (1997).

[63] Y. Harada and T. Asakura, Radiation forces on a dielectric sphere in the Rayleigh scattering regime, *Optics Communication* **124**, 529–541 (1996).

[64] A. Ashkin, Forces of a single-beam gradient laser trap on a dielectric sphere in the ray optics regime, *Biophysical Journal* **61**, 569–582 (1992).

[65] W. H. Wright, G. J. Sonek, and M. W. Berns, Radiation trapping forces on microspheres with optical tweezers, *Applied Physics Letters* **63**, 715–717 (1993).

[66] G. Gouesbet, B. Maheu, and G. Gréhan, Light scattering from a sphere arbitrarily located in a Gaussian beam, using a Bromwich formulation, *Journal of the Optical Society of America A* **5**, 1427–1443 (1988).

[67] M. Pitzek, R. Steiger, G. Thalhammer, S. Bernet, and M. Ritsch-Marte, Optical mirror trap with a large field of view, *Optics Express* **17**, 19414–19423 (2009).

[68] K. Svoboda and S. M. Block, Biological Applications of Optical Forces, *Annual Review of Biophysics and Biomolecular Structure* **23**, 247–285 (1994).

[69] K. C. Neuman, E. H. Chadd, G. F. Liou, K. Bergman, and S. M. Block, Characterization of photodamage to *Escherichia coli* in optical traps, *Biophysical Journal* **77**, 2856–2863 (1999).

[70] H. Liang, K. T. Vu, P. Krishnan, T. C. Trang, D. Shin, S. Kimel, and M. W. Berns, Wavelength dependence of cell cloning efficiency after optical trapping, *Biophysical Journal* **70**, 1529–1533 (1996).

[71] E. Eriksson, K. Sott, F. Lundqvist, M. Sveningsson, J. Scrimgeour, D. Hanstorp, M. Goksör, and A. Granéli, A microfluidic device for reversible environmental changes around single cells using optical tweezers for cell selection and positioning, *Lab on a Chip* **10**, 617–625 (2010).

[72] L. Bendrioua, M. Smedh, J. Almquist, M. Cvijovic, M. Jirstrand, M. Goksör, C. B. Adiels, and S. Hohmann, Yeast AMP-activated Protein Kinase Monitors Glucose Concentration Changes and Absolute Glucose Levels, *Journal of Biological Chemistry* **289**, 12863–12875 (2014).

[73] P. Tabeling, *Introduction to Microfluidics*, Oxford University Press, New York, USA (2005).

[74] D. J. Beebe, G. A. Mensing, and G. M. Walker, Physics and applications of microfluidics in biology, *Annual Review of Biomedical Engineering* **4**, 261–286 (2002).

[75] X. F. Peng and G. P. Peterson, Convective heat transfer and flow friction for water flow in microchannel structures, *International Journal of Heat and Mass Transfer* **39**, 2599–2608 (1996).

[76] C. Nordling and J. Österman, *Physics Handbook of Science and Engineering*, Studentlitteratur, Lund, Sweden (2004).

[77] C. T. Culbertson, S. C. Jacobson, and J. M. Ramsey, Diffusion coefficient measurements in microfluidic devices, *Talanta* **56**, 365–373 (2002).

[78] G. H. Patterson, S. M. Knobel, P. Arkhammar, O. Thastrup, and D. W. Piston, Separation of the glucose-stimulated cytoplasmic and mitochondrial NAD(P)H responses in pancreatic islet $\beta$ cells, *Proceedings of the National Academy of Sciences of the United States of America* **97**, 5203–5207 (2000).

[79] L. Bengtsson, *Electrical measurement systems and methods*, Studentlitteratur, Lund, Sweden (2014).

[80] M. G. Rosenblum, A. S. Pikovsky, and J. Kurths, Phase Synchronization of Chaotic Oscillators, *Physical Review Letters* **76**, 1804–1807 (1996).

[81] S. H. Strogatz, From Kuramoto to Crawford: exploring the onset of synchronization in populations of coupled oscillators, *Physica D* **143**, 1–20 (2000).

[82] A. Pikovsky, M. Rosenblum, and J. Kurths, *Synchronization: A universal concept in nonlinear sciences*, volume 12, Cambridge University Press, Cambridge, United Kingdom (2003).

[83] A. Goldbeter and R. Lefever, Dissipative structures for an allosteric model. Application to glycolytic oscillations, *Biophysical Journal* **12**, 1302–1315 (1972).

[84] K. Nielsen, P. G. Sørensen, F. Hynne, and H. G. Busse, Sustained oscillations in glycolysis: an experimental and theoretical study of chaotic and complex periodic behavior and of quenching of simple oscillations, *Biophysical Chemistry* **72**, 49–62 (1998).

[85] J. Wolf, J. Passarge, O. J. G. Somsen, J. L. Snoep, R. Heinrich, and H. V. Westerhoff, Transduction of Intracellular and Intercellular Dynamics in Yeast Glycolytic Oscillations, *Biophysical Journal* **78**, 1145–1153 (2000).

[86] B. Teusink, J. Passarge, C. A. Reijenga, E. Esgalhado, C. C. van der Weijden, M. Schepper, M. C. Walsh, B. M. Bakker, K. van Dam, H. V. Westerhoff, and J. L. Snoep, Can yeast glycolysis be understood in terms of in vitro kinetics of the constituent enzymes? Testing biochemistry, *European Journal of Biochemistry* **267**, 5313–5329 (2000).

[87] J. L. Snoep, F. Bruggeman, B. G. Olivier, and H. V. Westerhoff, Towards building the silicon cell: A modular approach, *BioSystems* **83**, 207–216 (2006).

[88] F. B. du Preez, D. D. van Niekerk, B. Kooi, J. M. Rohwer, and J. L. Snoep, From steady-state to synchronized yeast glycolytic oscillations I: model construction, *FEBS Journal* **279**, 2810–2822 (2012).

[89] F. B. du Preez, D. D. van Niekerk, and J. L. Snoep, From steady-state to synchronized yeast glycolytic oscillations II: model validation, *FEBS Journal* **279**, 2823–2836 (2012).

[90] P. Nelson, *Biological Physics*, W. H. Freeman and Company, New York, USA (2008).

[91] J. M. Thevelein and S. Hohmann, Trehalose synthase: guard to the gate of glycolysis in yeast?, *Trends in Biochemical Sciences* **20**, 3–10 (1995).

[92] B. O. Hald and P. G. Sørensen, Modeling Diauxic Glycolytic Oscillations in Yeast, *Biophysical Journal* **99**, 3191–3199 (2010).

[93] J. Wolf and R. Heinrich, Effect of cellular interaction on glycolytic oscillations in yeast: a theoretical investigation, *Biochemical Journal* **345**, 321–334 (2000).

[94] A. Weber, Y. Prokazov, W. Zuschratter, and M. J. B. Hauser, Desynchronisation of glycolytic oscillations in yeast cell populations, *PLOS One* **7**, e43276 (2012).

[95] B. Hess, The glycolytic oscillator, *Journal of Experimental Biology* **81**, 7–14 (1979).

[96] E. E. Sel'kov, Stabilization of Energy Charge, Generation of Oscillations and Multiple Steady States in Energy Metabolism as a Result of Purely Stoichiometric Regulation, *European Journal of Biochemistry* **59**, 151–157 (1975).

[97] P. D. Kourdis, R. Steuer, and D. A. Goussis, Physical understanding of complex multiscale biochemical models via algorithmic simplification: Glycolysis in Saccharomyces cerevisiae, *Physica D* **239**, 1798–1817 (2010).

[98] J. A. Burns, A. Cornish-Bowden, A. K. Groen, R. Heinrich, H. Kacser, J. W. Porteous, S. M. Rapoport, T. A. Rapoport, J. W. Stucki, J. M. Tager, R. J. A. Wanders, and H. V. Westerhoff, Control analysis of metabolic systems, *Trends in Biochemical Sciences* **10**, 16–16 (1985).

[99] K. A. Reijenga, Y. M. G. A. van Megen, B. W. Kooi, B. M. Bakker, J. L. Snoep, H. W. van Verseveld, and H. V. Westerhoff, Yeast glycolytic oscillations that are not controlled by a single oscillophore: a new definition of oscillophore strength, *Journal of Theoretical Biology* **232**, 385–398 (2005).

[100] M. A. Aon, S. Cortassa, H. V. Westerhoff, J. A. Berden, E. van Spronsen, and K. van Dam, Dynamic regulation of yeast glycolytic oscillations by mitochondrial functions, *Journal of Cell Science* **99**, 325–334 (1991).

[101] T. D. Schrøder, V. C. Özalp, A. Lunding, K. D. Jernshøj, and L. F. Olsen, An experimental study of the regulation of glycolytic oscillations in yeast, *FEBS Journal* **280**, 6033–6044 (2013).

[102] V. C. Özalp, T. R. Pedersen, L. J. Nielsen, and L. F. Olsen, Time-resolved Measurements of Intracellular ATP in the Yeast *Saccharomyces cerevisiae* using a New Type of Nanobiosensor, *The Journal of Biological Chemistry* **285**, 37579–37588 (2010).

[103] E. K. Pye, *Glycolytic oscillations in cells and extracts of yeast - some unsolved problems*, In: *Biological and Biochemical Oscillators*, (B. Chance, E. K. Pye, A. Ghosh, and B. Hess, Eds.), Academic Press, New York, USA (1973).

[104] P. H. Richter and J. Ross, Oscillations and efficiency in glycolysis, *Biophysical Chemistry* **12**, 285–297 (1980).